

COSMOLOGY: STANDARD AND INFLATIONARY *

Michael S. Turner

*Departments of Physics and Astronomy & Astrophysics,
Enrico Fermi Institute, The University of Chicago, Chicago, IL 60637-1433*

*NASA/Fermilab Astrophysics Center,
Fermi National Accelerator Laboratory, Batavia, IL 60510-0500*

Abstract

In these lectures I review the standard hot big-bang cosmology, emphasizing its successes, its shortcomings, and its major challenges—developing a detailed understanding of the formation of structure in the Universe and identifying the constituents of the ubiquitous dark matter. I then discuss the motivations for—and the fundamentals of—inflationary cosmology, particularly emphasizing the quantum origin of metric (density and gravity-wave) perturbations. Inflation addresses the shortcomings of the standard cosmology, specifies the nature of the dark matter, and provides the “initial data” for structure formation. I conclude by addressing the implications of inflation for structure formation and discussing the different versions of cold dark matter. The flood of data—from the Heavens and from Earth—should in the next decade test inflation and discriminate between the different cold dark matter models.

1 Hot Big Bang: Successes and Challenges

1.1 Successes

The hot big-bang model, more properly the Friedmann-Robertson-Walker (FRW) cosmology or standard cosmology, is spectacularly successful: In short, it provides a reliable and tested accounting of the history of the Universe from about 0.01 sec after the bang until today, some 15 billion years later. The primary pieces of evidence that support the model are: (1) The expansion of the Universe; (2) The cosmic background radiation (CBR); (3) The primordial abundances of the light elements D, ^3He , ^4He , and ^7Li [1]; and (4) The existence of small variations in the temperature of the CBR measured in different directions (of order $30\mu\text{K}$ on angular scales from 0.5° to 90°).

*Supported in part by the DOE (at Chicago and Fermilab) and by the NASA through grant NAG 5-2788 (at Fermilab).

Figure 1: Hubble diagram (from [3]). The deviation from a linear relationship around 40 Mpc is due to peculiar velocities.

1.1.1 The expansion

Although the precise value of the Hubble constant is not known to better than a factor of two, $H_0 = 100h \text{ km sec}^{-1} \text{ Mpc}^{-1}$ with $h = 0.4 - 0.9$, there is little doubt that the expansion obeys the “Hubble law” out to red shifts approaching unity [2, 3]; see Fig. 1. As is well appreciated, the fundamental difficulty in determining the Hubble constant is the calibration of the cosmic-distance scale as “standard candles” are required [4, 5]. The detection of Cepheid variable stars in an Virgo Cluster galaxy (M101) with the Hubble Space Telescope [6] was a giant step toward an accurate determination of H_0 , and the issue could well be settled within five years.

The Hubble law allows one to infer the distance to an object from its red shift z : $d = zH_0^{-1} \simeq 3000z h^{-1} \text{ Mpc}$ (for $z \ll 1$, the galaxy’s recessional velocity $v \simeq zc$), and hence “maps of the Universe” constructed from galaxy positions and red shifts are referred to as red-shift surveys. Ordinary galaxies and clusters of galaxies are seen out to red shifts of order unity; more unusual and rarer objects, such as radio galaxies and quasars, are seen out to red shifts of almost five (the current record holder is a quasar with red shift 4.9). Thus, we can probe the Universe with visible light to within a few billion years of the big bang.

1.1.2 The cosmic background radiation

The spectrum of the cosmic background radiation (CBR) is consistent that of a black body at temperature 2.73 K over more than three decades in wavelength ($\lambda \sim 0.03 \text{ cm} - 100 \text{ cm}$); see Fig. 2. The most accurate measurement of the temperature and spectrum is that by the FIRAS instrument on the COBE satellite which determined its temperature to be $2.726 \pm 0.005 \text{ K}$ [7]. It is difficult to come up with a process other than an early hot and dense phase in the history of the Universe that would lead to such a precise black body [8]. According to the standard cosmology, the surface of last scattering for the CBR is the Universe at a red shift of about 1100 and an age of about $180,000 (\Omega_0 h^2)^{-1/2} \text{ yrs}$. It is possible that the Universe became ionized again after this epoch, or due to energy injection never recombined; in this case the last-scattering surface is even “closer,” $z_{\text{LSS}} \simeq 10[\Omega_B h / \sqrt{\Omega_0}]^{-2/3}$.

The temperature of the CBR is very uniform across the sky, to better than a part in 10^4 on angular scales from arcminutes to 90 degrees; see Fig. 3. Three forms of temperature anisotropy—two spatial and one temporal—have now been detected: (1) A dipole anisotropy of about a part in 10^3 , generally believed to be due to the motion of galaxy relative to the cosmic rest frame, at a speed of about 620 km sec^{-1} [9]; (2) A yearly modulation in the temperature in a given direction on the sky of about a part in 10^4 , due to our orbital motion around the sun at 30 km sec^{-1} , see Fig. 4 [10]; and (3) The temperature anisotropies detected by the Differential Microwave Radiometer (DMR) on the Cosmic Background Explorer (COBE) satellite [11] and more than ten other experiments [12].

COBE has made the most precise measurement of CBR anisotropy, $\langle(\Delta T/T)^2\rangle_{10^\circ}^{1/2} = 1.1 \pm 0.1 \times 10^{-5}$ (the *rms* temperature fluctuation averaged over the entire sky as measured by a beam of width 10°). Other ground-based and balloon-borne instruments have now measured CBR anisotropy on angular scales from about 0.5° to 30° . The CBR anisotropy provides strong evidence for primeval density inhomogeneities of the same magnitude, which amplified by gravity, grew into the structures that we see today: galaxies, clusters of galaxies, superclusters, voids, walls, and so on. Moreover, CBR anisotropy measurements are beginning to map out the inhomogeneity on scales from about 100 Mpc to 10^4 Mpc .

1.1.3 Primordial nucleosynthesis

Last, but certainly not least, there are the abundance of the light elements. According to the standard cosmology, when the age of the Universe was measured in seconds, the temperatures were of order MeV, and the conditions were right for nuclear reactions which ultimately led to the synthesis of significant amounts of D, ^3He , ^4He , and ^7Li . The yields of primordial nucleosynthesis depend upon the baryon density, quantified as the baryon-to-photon ratio η , and the number of very light ($\lesssim \text{MeV}$) particle species, often quantified as the equivalent number of light neutrino species, N_ν . The predictions for the primordial abundances of all four light elements agree with their measured abundances provided that $2.5 \times 10^{-10} \lesssim \eta \lesssim 6 \times 10^{-10}$ and $N_\nu \lesssim 3.9$; see

Figure 2: (a) CBR spectrum as measured by the FIRAS on COBE; (b) Summary of other CBR temperature measurements. (Figure courtesy of G. Smoot.)

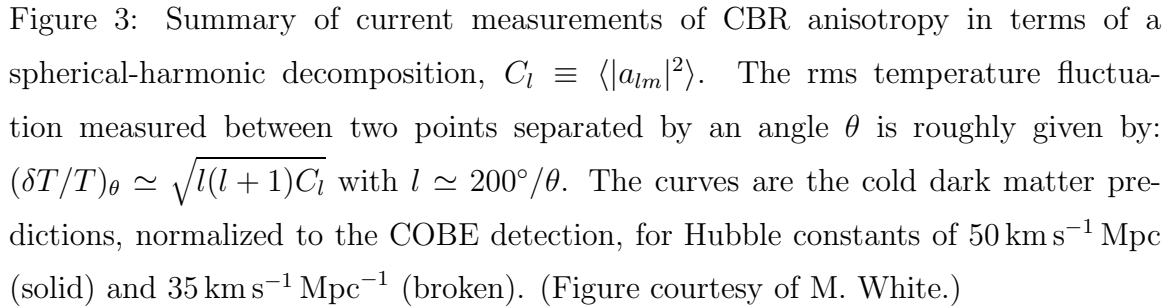


Figure 3: Summary of current measurements of CBR anisotropy in terms of a spherical-harmonic decomposition, $C_l \equiv \langle |a_{lm}|^2 \rangle$. The rms temperature fluctuation measured between two points separated by an angle θ is roughly given by: $(\delta T/T)_\theta \simeq \sqrt{l(l+1)C_l}$ with $l \simeq 200^\circ/\theta$. The curves are the cold dark matter predictions, normalized to the COBE detection, for Hubble constants of $50 \text{ km s}^{-1} \text{ Mpc}$ (solid) and $35 \text{ km s}^{-1} \text{ Mpc}^{-1}$ (broken). (Figure courtesy of M. White.)

Figure 4: Yearly modulation of the CBR temperature—the earth really orbits the sun(!) (from [10]).

Fig. 5 [13, 14, 15, 16].

Accepting the success of the standard model of nucleosynthesis, our precise knowledge of the present temperature of the Universe allows us to convert η to a mass density, and by dividing by the critical density, $\rho_{\text{crit}} \simeq 1.88h^2 \times 10^{-29} \text{ g cm}^{-3}$, to the fraction of critical density contributed by ordinary matter:

$$0.009 \lesssim \Omega_B h^2 \lesssim 0.022; \quad \Rightarrow \quad 0.01 \lesssim \Omega_B \lesssim 0.15; \quad (1)$$

this is the most accurate determination of the baryon density. Note, the uncertainty in the value of the Hubble constant leads to most of the uncertainty in Ω_B .

The nucleosynthesis bound to N_ν , and more generally to the number of light degrees of freedom in thermal equilibrium at the epoch of nucleosynthesis, is consistent with precision measurements of the properties of the Z^0 boson, which give $N_\nu = 3.0 \pm 0.02$; further, the cosmological bound predates these accelerator measurements! The nucleosynthesis bound provides a stringent limit to the existence of new, light particles (even beyond neutrinos), and even provides a bound to the mass the tau neutrino, excluding a long-lived tau-neutrino of mass between 0.5 MeV and 30 MeV [17, 18]. Primordial nucleosynthesis provides a beautiful illustration of the powers of the Heavenly Laboratory, though it is outside the focus of these lectures.

The remarkable success of primordial nucleosynthesis gives us confidence that the standard cosmology provides an accurate accounting of the Universe at least as early as 0.01 sec after the bang, when the temperature was about 10 MeV.

1.1.4 Et cetera—and the age crisis?

There are additional lines of reasoning and evidence that support the standard cosmology [8]. I mention two: the age of the Universe and structure formation. I will discuss the basics of structure formation a bit later; for now it suffices to say that the standard cosmology provides a basic framework for understanding the formation of structure—amplification of small primeval density inhomogeneities through gravitational instability. Here I focus on the age of the Universe.

The expansion age of the Universe—time back to zero size—depends upon the present expansion rate, energy content, and equation of state: $t_{\text{exp}} = f(\rho, p)H_0^{-1} \simeq 9.8h^{-1}f(\rho, p) \text{ Gyr}$. For a matter-dominated Universe, f is between 1 and 2/3 (for Ω_0 between 0 and 1), so that the expansion age is somewhere between 7 Gyr and 20 Gyr. There are other independent measures of the age of the Universe, e.g., based upon long-lived radioisotopes, the oldest stars, and the cooling of white dwarfs. These “ages,” ranging from 13 to 18 Gyr, span the same interval(!) [19]. This wasn’t always the case; as late as the early 1950’s it was believed that the Hubble constant was $500 \text{ km sec}^{-1} \text{ Mpc}^{-1}$, implying an expansion age of at most 2 Gyr—less than the age of the earth. This discrepancy was an important motivation for the steady-state cosmology.

While there is *general* agreement between the expansion age and other determinations of the age of the Universe, some cosmologists are worried that cosmology is on

Figure 5: Predicted light-element abundances including 2σ theoretical uncertainties (from [14]). The inferred primordial abundances and concordance regions are indicated.

the verge of another age crisis [5]. Let me explain, while Sandage and a few others continue to obtain values for the Hubble constant around $50 \text{ km s}^{-1} \text{ Mpc}^{-1}$ [2], a variety of different techniques seem to be converging on a value around $80 \pm 10 \text{ km s}^{-1} \text{ Mpc}^{-1}$ [5]. If $H_0 = 80 \text{ km s}^{-1} \text{ Mpc}^{-1}$, then $t_{\text{exp}} = 12f(\rho, p) \text{ Gyr}$, and for $\Omega_0 = 1$, $t_{\text{exp}} = 8 \text{ Gyr}$, which is clearly inconsistent with other measures of the age. If $H_0 = 80 \text{ km s}^{-1} \text{ Mpc}^{-1}$, one is almost forced to consider the radical alternative of a cosmological constant. For example, even with $\Omega_0 = 0.2$, $f \simeq 0.85$, corresponding to $t_{\text{exp}} \simeq 10 \text{ Gyr}$; on the other hand, for a flat Universe with $\Omega_\Lambda = 0.7$, $f \simeq 1$ and the expansion age $t_{\text{exp}} \simeq 12 \text{ Gyr}$. As I shall discuss later, structure formation provides another motivation for a cosmological constant. As mentioned earlier, the detection of Cepheid variables in Virgo [6] is a giant step toward an accurate determination of H_0 , and it seems likely that the issue may be settled soon.

1.2 Basics of the Big Bang Model

The standard cosmology is based upon the maximally spatially symmetric Robertson-Walker line element

$$ds^2 = dt^2 - R(t)^2 \left[\frac{dr^2}{1 - kr^2} + r^2(d\theta^2 + \sin^2\theta d\phi^2) \right]; \quad (2)$$

where $R(t)$ is the cosmic-scale factor, $R_{\text{curv}} \equiv R(t)|k|^{-1/2}$ is the curvature radius, and $k/|k| = -1, 0, 1$ is the curvature signature. All three models are without boundary: the positively curved model is finite and “curves” back on itself; the negatively curved and flat models are infinite in extent (though finite versions of both can be constructed by imposing a periodic structure: identifying all points in space with a fundamental cube). The Robertson-Walker metric embodies the observed isotropy and homogeneity of the Universe. It is interesting to note that this form of the line element was originally introduced for sake of mathematical simplicity; we now know that it is well justified at early times or today on large scales ($\gg 10 \text{ Mpc}$), at least within our Hubble volume.

The coordinates, r , θ , and ϕ , are referred to as comoving coordinates: A particle at rest in these coordinates remains at rest, i.e., constant r , θ , and ϕ . A freely moving particle eventually comes to rest these coordinates, as its momentum is red shifted by the expansion, $p \propto R^{-1}$. Motion with respect to the comoving coordinates (or cosmic rest frame) is referred to as peculiar velocity; unless “supported” by the inhomogeneous distribution of matter peculiar velocities decay away as R^{-1} . Thus the measurement of peculiar velocities, which is not easy as it requires independent measures of both the distance and velocity of an object, can be used to probe the distribution of mass in the Universe.

Physical separations (i.e., measured by meter sticks) between freely moving particles scale as $R(t)$; or said another way the physical separation between two points is simply $R(t)$ times the coordinate separation. The momenta of freely propagating particles decrease, or “red shift,” as $R(t)^{-1}$, and thus the wavelength of a photon

stretches as $R(t)$, which is the origin of the cosmological red shift. The red shift suffered by a photon emitted from a distant galaxy $1+z = R_0/R(t)$; that is, a galaxy whose light is red shifted by $1+z$, emitted that light when the Universe was a factor of $(1+z)^{-1}$ smaller. Thus, when the light from the most distant quasar yet seen ($z = 4.9$) was emitted the Universe was a factor of almost six smaller; when CBR photons last scattered the Universe was about 1100 times smaller.

1.2.1 Friedmann equation and the First Law

The evolution of the cosmic-scale factor is governed by the Friedmann equation

$$H^2 \equiv \left(\frac{\dot{R}}{R}\right)^2 = \frac{8\pi G \rho_{\text{tot}}}{3} - \frac{k}{R^2}; \quad (3)$$

where ρ_{tot} is the total energy density of the Universe, matter, radiation, vacuum energy, and so on. A cosmological constant is often written as an additional term ($= \Lambda/3$) on the rhs; I will choose to treat it as a constant energy density (“vacuum-energy density”), where $\rho_{\text{vac}} = \Lambda/8\pi G$. (My convention in this regard is not universal.) The evolution of the energy density of the Universe is governed by

$$d(\rho R^3) = -p dR^3; \quad (4)$$

which is the First Law of Thermodynamics for a fluid in the expanding Universe. (In the case that the stress energy of the Universe is comprised of several, noninteracting components, this relation applies to each separately; e.g., to the matter and radiation separately today.) For $p = \rho/3$, ultra-relativistic matter, $\rho \propto R^{-4}$; for $p = 0$, very nonrelativistic matter, $\rho \propto R^{-3}$; and for $p = -\rho$, vacuum energy, $\rho = \text{const.}$ If the rhs of the Friedmann equation is dominated by a fluid with equation of state $p = \gamma\rho$, it follows that $\rho \propto R^{-3(1+\gamma)}$ and $R \propto t^{2/3(1+\gamma)}$.

We can use the Friedmann equation to relate the curvature of the Universe to the energy density and expansion rate:

$$\frac{k/R^2}{H^2} = \Omega - 1; \quad \Omega = \frac{\rho_{\text{tot}}}{\rho_{\text{crit}}}; \quad (5)$$

and the critical density today $\rho_{\text{crit}} = 3H^2/8\pi G = 1.88h^2 \text{ g cm}^{-3} \simeq 1.05 \times 10^4 \text{ eV cm}^{-3}$. There is a one to one correspondence between Ω and the spatial curvature of the Universe: positively curved, $\Omega_0 > 1$; negatively curved, $\Omega_0 < 1$; and flat ($\Omega_0 = 1$). Further, the “fate of the Universe” is determined by the curvature: model universes with $k \leq 0$ expand forever, while those with $k > 0$ necessarily recollapse. The curvature radius of the Universe is related to the Hubble radius and Ω by

$$R_{\text{curv}} = \frac{H^{-1}}{|\Omega - 1|^{1/2}}. \quad (6)$$

In physical terms, the curvature radius sets the scale for the size of spatial separations where the effects of curved space become “pronounced.” And in the case of the positively curved model it is just the radius of the 3-sphere.

The energy content of the Universe consists of matter and radiation (today, photons and neutrinos). Since the photon temperature is accurately known, $T_0 = 2.73 \pm 0.01$ K, the fraction of critical density contributed by radiation is also accurately known: $\Omega_{\text{rad}} h^2 = 4.18 \times 10^{-5}$. The matter content is another matter.

1.2.2 A short diversion concerning the present mass density

The matter density today, i.e., the value of Ω_0 , is not nearly so well known [20]. Stars contribute much less than 1% of critical density; based upon nucleosynthesis, we can infer that baryons contribute between 1% and 15% of critical. The dynamics of various systems allow astronomers to infer their gravitational mass. With their telescopes they measure the amount of light, and form a mass-to-light ratio. Multiplying this by the measured luminosity density of the Universe gives a determination of the mass density. (The critical mass-to-light ratio is $1200 h M_\odot / \mathcal{L}_\odot$.)

The motions of stars and gas clouds in spiral galaxies indicate that most of the mass of spiral galaxies exists in the form of dark (i.e., no detectable radiation), extended halos, whose full extent is still not known. Many cite the flat rotation curves of spiral galaxies, which indicate that the halo density decreases as r^{-2} , as the best evidence that most of the matter in the Universe is dark. Taking the mass-to-light ratio inferred for spiral galaxies to be typical of the Universe as a whole and remembering that the full extent of the dark matter halos is not known, one infers $\Omega_{\text{halo}} \gtrsim 0.03 - 0.1$ [21].

The masses of clusters of galaxies have been determined by applying the virial theorem to the motions of member galaxies or to the hot gas that fills the intracluster medium, and by the analyzing (weak) gravitational lensing of very distant galaxies by clusters. These mass estimates too indicate the presence of large amounts of dark matter; when more than one method is applied to the same cluster the mass estimates are consistent. Taking cluster mass-to-light ratios to be typical of the Universe as a whole, in spite of the fact that only about 1 in 10 galaxies resides in a cluster, one infers $\Omega_{\text{cluster}} \sim 0.2 - 0.4$.

Another interesting fact has been learned from x-ray observations of clusters: the ratio of baryons in the hot intracluster gas to the total cluster mass, $M_{\text{gas}}/M_{\text{tot}} \simeq (0.04 - 0.08) h^{-3/2}$ [22]. Since the gas mass is much greater than the mass in the visible galaxies, this ratio provides an estimate of the cluster baryon fraction, *provided that most of the baryons reside in the hot gas or in galaxies*, and suggests that the bulk of matter in clusters is in a form other than baryons!

Not one of these methods is wholly satisfactory: Rotation curves of spiral galaxies are still “flat” at the last measured points, indicating that the mass is still increasing; likewise, cluster virial mass estimates are insensitive to material that lies beyond the region occupied by the visible galaxies—and moreover, only about one galaxy in ten

resides in a cluster. What one would like is a measurement of the mass of a very big sample of the Universe, say a cube of $100h^{-1}$ Mpc on a side, which contains tens of thousands of galaxies.

Over the past five years or so progress has been made toward such a measurement. It involves the peculiar motion of our own galaxy, at a speed of about 620 km sec^{-1} in the general direction of Hydra-Centaurus. This motion is due to the lumpy distribution of matter in our vicinity. By using gravitational-perturbation theory (actually, not much more than Newtonian physics) and the distribution of galaxies in our vicinity (as determined by the IRAS catalogue of infrared selected galaxies), one can infer the average mass density in a very large volume and thereby Ω_0 .

The basic physics behind the method is simple: the net gravitational pull on our galaxy depends both upon how inhomogeneous the distribution of galaxies is and how much mass is associated with each galaxy; by measuring the distribution of galaxies and our peculiar velocity one can infer the “mass per galaxy” and Ω_0 .

The value that has been inferred is big(!)—close to unity— and provides a very strong case that Ω_0 is at least 0.3 [23]. Moreover, the measured peculiar velocities of other galaxies in this volume, more than thousand, have been used in a similar manner and indicate a similarly large value for Ω_0 [24]. While this technique is very powerful, it does have its drawbacks: One has to make simple assumptions about how accurately mass is traced by light (the observed galaxies); one has to worry whether or not a significant portion of our galaxy’s velocity is due to galaxies outside the IRAS sample—if so, this would lead to an overestimate of Ω_0 ; and so on. This technique is not only very promising—but provides the “correct” answer (in my opinion!).

The so-called classical kinematic tests—Hubble diagram, angle-red shift relation, galaxy count-red shift relation—can, in principle, provide a determination of Ω_0 by determining the deceleration parameter q_0 [25]. However, all these methods require standard candles, rulers, or galaxies, and for this reason have proved inconclusive. However, that hasn’t discouraged everyone. There are a number of efforts to determine q_0 using the galaxy number-count test [26], and two groups are trying to measure q_0 by constructing a Hubble diagram based upon Type Ia supernovae (out to redshifts of 0.5 or more).

To summarize this aside on the mass density of the Universe:

1. Most of the matter is dark.
2. Baryons provide between about 1% and 15% of the mass density (allowing $0.4 < h < 1$; taking $h > 0.6$ the upper limit decreases to 6%).
3. There is a strong case that $\Omega_0 \gtrsim 0.3$ (peculiar velocities); a convincing case that $\Omega_0 \gtrsim 0.2$ (cluster masses); and an airtight case that $\Omega_0 \gtrsim 0.1$ (flat rotation curves of spirals).
4. Most of the baryons are dark (not in stars). In clusters the bulk of the baryons are in hot gas.

5. The evidence for nonbaryonic dark matter continues to mount; e.g., the gap between Ω_B and Ω_0 and the cluster baryon fraction.

The current prejudice—and certainly that of this author—is a flat Universe ($\Omega_0 = 1$) with nonbaryonic dark matter, $\Omega_X \sim 1 \gg \Omega_B$. However, I shall continue to display the Ω_0 dependence of important quantities.

1.2.3 The early, radiation-dominated Universe

In any case, at present, matter outweighs radiation by a wide margin. However, since the energy density in matter decreases as R^{-3} , and that in radiation as R^{-4} (the extra factor due to the red shifting of the energy of relativistic particles), at early times the Universe was radiation dominated—indeed the calculations of primordial nucleosynthesis provide excellent evidence for this. Denoting the epoch of matter-radiation equality by subscript ‘EQ,’ and using $T_0 = 2.73$ K, it follows that

$$R_{\text{EQ}} = 4.18 \times 10^{-5} (\Omega_0 h^2)^{-1}; \quad T_{\text{EQ}} = 5.62 (\Omega_0 h^2) \text{ eV}; \quad (7)$$

$$t_{\text{EQ}} = 4.17 \times 10^{10} (\Omega_0 h^2)^{-2} \text{ sec}. \quad (8)$$

At early times the expansion rate and age of the Universe were determined by the temperature of the Universe and the number of relativistic degrees of freedom:

$$\rho_{\text{rad}} = g_*(T) \frac{\pi^2 T^4}{30}; \quad H \simeq 1.67 g_*^{1/2} T^2 / m_{\text{Pl}}; \quad (9)$$

$$\Rightarrow R \propto t^{1/2}; \quad t \simeq 2.42 \times 10^{-6} g_*^{-1/2} (T / \text{GeV})^{-2} \text{ sec}; \quad (10)$$

where $g_*(T)$ counts the number of ultra-relativistic degrees of freedom (\approx the sum of the internal degrees of freedom of particle species much less massive than the temperature) and $m_{\text{Pl}} \equiv G^{-1/2} = 1.22 \times 10^{19} \text{ GeV}$ is the Planck mass. For example, at the epoch of nucleosynthesis, $g_* = 10.75$ assuming three, light ($\ll \text{MeV}$) neutrino species; taking into account all the species in the standard model, $g_* = 106.75$ at temperatures much greater than 300 GeV; see Fig. 6.

A quantity of importance related to g_* is the entropy density in relativistic particles,

$$s = \frac{\rho + p}{T} = \frac{2\pi^2}{45} g_* T^3,$$

and the entropy per comoving volume,

$$S \propto R^3 s \propto g_* R^3 T^3.$$

By a wide margin most of the entropy in the Universe exists in the radiation bath. The entropy density is proportional to the number density of relativistic particles. At present, the relativistic particle species are the photons and neutrinos, and the

Figure 6: The total effective number of relativistic degrees of freedom $g_*(T)$ in the standard model of particle physics as a function of temperature.

entropy density is a factor of 7.04 times the photon-number density: $n_\gamma = 413 \text{ cm}^{-3}$ and $s = 2905 \text{ cm}^{-3}$.

In thermal equilibrium—which provides a good description of most of the history of the Universe—the entropy per comoving volume S remains constant. This fact is very useful. First, it implies that the temperature and scale factor are related by

$$T \propto g_*^{-1/3} R^{-1}, \quad (11)$$

which for $g_* = \text{const}$ leads to the familiar $T \propto R^{-1}$.

Second, it provides a way of quantifying the net baryon number (or any other particle number) per comoving volume:

$$N_B \equiv R^3 n_B = \frac{n_B}{s} \simeq (4 - 7) \times 10^{-11}. \quad (12)$$

The baryon number of the Universe tells us two things: (1) the entropy per particle in the Universe is extremely high, about 10^{10} or so compared to about 10^{-2} in the sun and a few in the core of a newly formed neutron star. (2) The asymmetry between matter and antimatter is very small, about 10^{-10} , since at early times quarks and antiquarks were roughly as abundant as photons. One of the great successes of particle cosmology is baryogenesis, the idea that B , C , and CP violating interactions occurring out-of-equilibrium early on allow the Universe to develop a net baryon number of this magnitude [27].

Finally, the constancy of the entropy per comoving volume allows us to characterize the size of comoving volume corresponding to our present Hubble volume in a very physical way: by the entropy it contains,

$$S_U = \frac{4\pi}{3} H_0^{-3} s \simeq 10^{90}. \quad (13)$$

1.2.4 The earliest history

The standard cosmology is tested back to times as early as about 0.01 sec; it is only natural to ask how far back one can sensibly extrapolate. Since the fundamental particles of Nature are point-like quarks and leptons whose interactions are perturbatively weak at energies much greater than 1 GeV, one can imagine extrapolating as far back as the epoch where general relativity becomes suspect, i.e., where quantum gravitational effects are likely to be important: the Planck epoch, $t \sim 10^{-43} \text{ sec}$ and $T \sim 10^{19} \text{ GeV}$. Of course, at present, our firm understanding of the elementary particles and their interactions only extends to energies of the order of 100 GeV, which corresponds to a time of the order of 10^{-11} sec or so. We can be relatively certain that at a temperature of 100 MeV – 200 MeV ($t \sim 10^{-5} \text{ sec}$) there was a transition (likely a second-order phase transition) from quark/gluon plasma to very hot hadronic matter, and that some kind of phase transition associated with the symmetry breakdown of the electroweak theory took place at a temperature of the order of 300 GeV ($t \sim 10^{-11} \text{ sec}$).

It is interesting to look at the progress that has taken place since Weinberg's classic text on cosmology was published in 1972 [28]; at that time many believed that the Universe had a limiting temperature of the order of several hundred MeV, due to the exponentially rising number of particle states, and that one could not speculate about earlier times. Today, based upon our present knowledge of physics and powerful mathematical tools (e.g., gauge theories, grand unified theories, and superstring theory) we are able to make quantitative speculations back to the Planck epoch—and even earlier. Of course, these speculations could be totally wrong, based upon a false sense of confidence (arrogance?). As I shall discuss, inflation is one of these well defined—and well motivated—speculations about the history of the Universe well after the Planck epoch, but well before primordial nucleosynthesis.

1.2.5 The matter and curvature dominated epochs

After the equivalence epoch, the matter density exceeds that of radiation. During the matter-dominated epoch the scale factor grows as $t^{2/3}$ and the age of the Universe is related to red shift by

$$t = 2.06 \times 10^{17} (\Omega_0 h^2)^{-1/2} (1+z)^{-3/2} \text{ sec.} \quad (14)$$

If $\Omega_0 < 1$, the matter-dominated epoch is followed by a “curvature-dominated” epoch where the rhs of the Friedmann equation is dominated by the $|k|/R^2$ term. When the Universe is curvature dominated it is said to expand freely, no longer decelerating since the gravitational effect of matter has become negligible: $\ddot{R} \approx 0$ and $R \propto t$. The epoch of curvature dominance begins when the matter and curvature terms are equal:

$$R_{\text{CD}} = \frac{\Omega_0}{1 - \Omega_0} \longrightarrow \Omega_0; \quad z_{\text{CD}} = \Omega_0^{-1} - 2 \longrightarrow \Omega_0^{-1}; \quad (15)$$

where the limits shown are for $\Omega_0 \rightarrow 0$. By way of comparison, in a flat Universe with a cosmological constant, the Universe becomes “vacuum dominated” when $R = R_{\text{vac}}$:

$$R_{\text{vac}} = \left(\frac{\Omega_0}{1 - \Omega_0} \right)^{1/3} \longrightarrow \Omega_0^{1/3}; \quad z_{\text{vac}} = \left(\frac{1 - \Omega_0}{\Omega_0} \right)^{1/3} - 1 \longrightarrow \Omega_0^{-1/3}. \quad (16)$$

For a given value of Ω_0 , the transition occurs much more recently, which has important implications for structure formation since small density perturbations only grow during the matter-dominated era.

1.2.6 One last thing: horizons

In spite of the fact that the Universe was vanishingly small at early times, the rapid expansion precluded causal contact from being established throughout. Photons travel

on null paths characterized by $dr = dt/R(t)$; the physical distance that a photon could have traveled since the bang until time t , the distance to the horizon, is

$$\begin{aligned} d_H(t) &= R(t) \int_0^t \frac{dt'}{R(t')} \\ &= t/(1-n) = nH^{-1}/(1-n) \quad \text{for } R(t) \propto t^n, \quad n < 1. \end{aligned} \quad (17)$$

Note, in the standard cosmology the distance to the horizon is finite, and up to numerical factors, equal to the age of the Universe or the Hubble radius, H^{-1} . For this reason, I will use horizon and Hubble radius interchangeably.¹

An important quantity is the entropy within a horizon volume: $S_{\text{HOR}} \sim H^{-3}T^3$; during the radiation-dominated epoch $H \sim T^2/m_{\text{Pl}}$, so that

$$S_{\text{HOR}} \sim \left(\frac{m_{\text{Pl}}}{T} \right)^3; \quad (18)$$

from this we conclude that at early times the comoving volume that encompasses all that we can see today (characterized by an entropy of 10^{90}) was comprised of a very large number of causally disconnected regions.

1.3 Two challenges: dark matter and structure formation

These two challenges are not unrelated: a detailed understanding of the formation of structure in the Universe necessarily requires knowledge of the quantity and composition of matter in the Universe.

We have every indication that the Universe at early times, say $t \ll 300,000$ yrs, was very homogeneous; however, today inhomogeneity (or structure) is ubiquitous: stars ($\delta\rho/\rho \sim 10^{30}$), galaxies ($\delta\rho/\rho \sim 10^5$), clusters of galaxies ($\delta\rho/\rho \sim 10 - 10^3$), superclusters, or “clusters of clusters” ($\delta\rho/\rho \sim 1$), voids ($\delta\rho/\rho \sim -1$), great walls, and so on.

For some 25 years the standard cosmology has provided a general framework for understanding this: Once the Universe becomes matter dominated (around 1000 yrs after the bang) primeval density inhomogeneities ($\delta\rho/\rho \sim 10^{-5}$) are amplified by gravity and grow into the structure we see today [29]. The fact that a fluid of self-gravitating particles is unstable to the growth of small inhomogeneities was first pointed out by Jeans and is known as the Jeans instability. The existence of these inhomogeneities was confirmed in spectacular fashion by the COBE DMR discovery of CBR anisotropy.

¹In inflationary models the horizon and Hubble radius are not roughly equal as the horizon distance grows exponentially relative to the Hubble radius; in fact, at the end of inflation they differ by e^N , where N is the number of e-folds of inflation. However, I will slip and use “horizon” and “Hubble radius” interchangeably, though I will always mean Hubble radius.

At last, the basic picture has been put on firm ground (whew!). Now the challenge is to fill in the details—origin of the density perturbations, precise evolution of the structure, and so on. As I shall emphasize, such an understanding may well be within reach, and offers a window on the early Universe.

1.3.1 The general picture: gravitational instability

Let us begin by expanding the perturbation to the matter density in plane waves

$$\frac{\delta\rho_M(\mathbf{x}, t)}{\rho_M} = \frac{1}{(2\pi)^3} \int d^3k \delta_k(t) e^{-i\mathbf{k}\cdot\mathbf{x}}, \quad (19)$$

where $\lambda = 2\pi/k$ is the comoving wavelength of the perturbation and $\lambda_{\text{phys}} = R\lambda$ is the physical wavelength. The comoving wavelengths of perturbations corresponding to bright galaxies, clusters, and the present horizon scale are respectively: about 1 Mpc, 10 Mpc, and $3000h^{-1}$ Mpc, where $1 \text{ Mpc} \simeq 3.09 \times 10^{24} \text{ cm} \simeq 1.56 \times 10^{38} \text{ GeV}^{-1}$.

The growth of small matter inhomogeneities of wavelength smaller than the Hubble scale ($\lambda_{\text{phys}} \lesssim H^{-1}$) is governed by a Newtonian equation:

$$\ddot{\delta}_k + 2H\dot{\delta}_k + v_s^2 k^2 \delta_k / R^2 = 4\pi G \rho_M \delta_k, \quad (20)$$

where $v_s^2 = dp/d\rho_M$ is the square of the sound speed. Competition between the pressure term and the gravity term on the rhs determine whether or not pressure can counteract gravity: Perturbations with wavenumber larger than the Jeans wavenumber, $k_J^2 = 4\pi G R^2 \rho_M / v_s^2$, are Jeans stable and just oscillate; perturbations with smaller wavenumber are Jeans unstable and can grow. For cold dark matter $v_s \simeq 0$ and all scales are Jeans unstable; even for baryonic matter, after decoupling k_J corresponds to a baryon mass of only about $10^5 M_\odot$. All the scales of interest here are Jeans unstable and we will ignore the pressure term.

Let us discuss solutions to this equation under different circumstances. First, consider the Jeans problem, evolution of perturbations in a static fluid, i.e., $H = 0$. In this case Jeans unstable perturbations grow exponentially, $\delta_k \propto \exp(t/\tau)$ where $\tau = 1/\sqrt{4\pi G \rho_M}$. Next, consider the growth of Jeans unstable perturbations in a matter-dominated Universe, i.e., $H^2 = 8\pi G \rho_M / 3$ and $R \propto t^{2/3}$. Because the expansion tends to “pull particles away from one another,” the growth is only power law, $\delta_k \propto t^{2/3}$; i.e., at the same rate as the scale factor. Finally, consider a radiation or curvature dominated Universe, i.e., $8\pi G \rho_{\text{rad}} / 3$ or $|k|/R^2$ much greater than $8\pi G \rho_M / 3$. In this case, the expansion is so rapid that matter perturbations grow very slowly, as $\ln R$ in radiation-dominated epoch, or not at all $\delta_k = \text{const}$ in the curvature-dominated epoch.

The growth of nonlinear perturbations is another matter; once a perturbation reaches an overdensity of order unity or larger it “separates” from the expansion—i.e., becomes its own self-gravitating system and ceases to expand any further. In the process of virial relaxation, its size decreases by a factor of two—density increases by

a factor of 8; thereafter, its density contrast grows as R^3 since the average matter density is decreasing as R^{-3} , though smaller scales could become Jeans unstable and collapse further to form smaller objects of higher density, stars, etc.

From this we learn that structure formation begins when the Universe becomes matter dominated and ends when it becomes curvature dominated (at least the growth of linear perturbations). The total growth available for linear perturbations is $R_{\text{CD}}/R_{\text{EQ}} \simeq 2.4 \times 10^4 \Omega_0^2 h^2$; since nonlinear structures have evolved by the present epoch, we can infer that primeval perturbations of the order $(\delta\rho_M/\rho_M)_{\text{EQ}} \sim 4 \times 10^{-5} (\Omega_0 h)^{-2}$ are required. Note that in a low-density Universe larger initial perturbations are necessary as there is less time for growth (“the low Ω_0 squeeze”). Further, in a baryon-dominated Universe things are even more difficult as perturbations in the baryons cannot begin to grow until after decoupling since matter is tightly coupled to the radiation. (In a flat, low- Ω_0 model with a cosmological constant the growth of linear fluctuations continues until almost today since $z_\Lambda \sim \Omega_0^{-1/3}$, and so the total growth factor is about $2.4 \times 10^4 (\Omega_0 h^2)$. We will return to this model later.)

1.3.2 CBR temperature fluctuations

The existence of density inhomogeneities has another important consequence: fluctuations in the temperature of the CBR of a similar amplitude [30]. The temperature difference measured between two points separated by a large angle ($\gtrsim 1^\circ$) arises due to a very simple physical effect:² The difference in the gravitational potential between the two points on the last-scattering surface, which in turn is related to the density perturbation, determines the temperature anisotropy on the angular scale subtended by that length scale,

$$\left(\frac{\delta T}{T}\right)_\theta = -\left(\frac{\delta\phi}{3}\right)_\lambda \approx \frac{1}{2} \left(\frac{\delta\rho}{\rho}\right)_{\text{HOR},\lambda}; \quad (21)$$

where the scale $\lambda \sim 100h^{-1} \text{Mpc}(\theta/\text{deg})$ subtends an angle θ on the last-scattering surface. This is known as the Sachs-Wolfe effect [31].

The quantity $(\delta\rho/\rho)_{\text{HOR},\lambda}$ is the amplitude with which a density perturbation crosses inside the horizon, i.e., when $R\lambda \sim H^{-1}$. Since the fluctuation in the gravitational potential $\delta\phi \sim (R\lambda/H^{-1})^2(\delta\rho/\rho)$, the horizon-crossing amplitude is equal to the gravitational potential (or curvature) fluctuation. The horizon-crossing amplitude $(\delta\rho/\rho)_{\text{HOR}}$ has several nice features: (i) during the matter-dominated era the potential fluctuation on a given scale remains constant, and thus the potential fluctuations at decoupling on scales that crossed inside the horizon after matter-radiation equality, corresponding to angular scales $\lesssim 0.1^\circ$, are just given by their horizon-crossing amplitude; (ii) because of its relationship to $\delta\phi$ it provides a dimensionless, geometrical

²Large angles mean those larger than the angle subtended by the horizon-scale at decoupling, $\theta \sim H_{\text{DEC}}^{-1}/H_0^{-1} \sim z_{\text{DEC}}^{-1/2} \sim 1^\circ$.

measure of the size of the density perturbation on a given scale, and its effect on the CBR; (iii) by specifying perturbation amplitudes at horizon crossing one can effectively avoid discussing the evolution of density perturbations on scales larger than the horizon, where a Newtonian analysis does not suffice and where gauge subtleties (associated with general relativity) come into play; and finally (iv) the density perturbations generated in inflationary models are characterized by $(\delta\rho/\rho)_{\text{HOR}} \simeq \text{const.}$

On angular scales smaller than about 1° two other physical effects lead to CBR temperature fluctuations: the motion of the last-scattering surface (Doppler) and the intrinsic fluctuations in the local photon temperature. These fluctuations are much more difficult to compute, and depend on microphysics—the ionization history of the Universe and the damping of perturbations in the photon-baryon fluid due to photon streaming. Not only are the Sachs-Wolfe fluctuations simpler to compute, but they accurately mirror the primeval fluctuations since at the epoch of decoupling microphysics is restricted to angular scales less than about a degree.

In sum, on large angular scales the Sachs-Wolfe effect dominates; on the scale of about 1° the total CBR fluctuation is about twice that due to the Sachs-Wolfe effect; on smaller scales the Doppler and intrinsic fluctuations dominate (see Fig. 3). CBR temperature fluctuations on scales smaller than about 0.1° are severely reduced by the smearing effect of the finite thickness of last-scattering surface. (For a beautiful exposition of how CBR anisotropy arises see Ref. [32].)

Details aside, in the context of the gravitational instability scenario density perturbations of sufficient amplitude to explain the observed structure lead to temperature fluctuations in the CBR of characteristic size,

$$\frac{\delta T}{T} \approx 10^{-5} (\Omega_0 h)^{-2}. \quad (22)$$

To be sure I have brushed over important details, but this equation conveys a great deal. First, the overall amplitude is set by the inverse of the growth factor, which is just the ratio of the radiation energy density to matter density at present. Next, it explains why theoretical cosmologists were so relieved when the COBE DMR detected temperature fluctuations of this amplitude, and conversely why one heard offhanded remarks before the COBE DMR detection that the standard cosmology was in trouble because the CBR temperature was too uniform to allow for the observed structure to develop. Finally, it illustrates one of the reasons why cosmologists who study structure formation have embraced the flat-Universe model with such enthusiasm: If we accept the Universe that meets the eye, $\Omega_0 \sim 0.1$ and baryons only, then the simplest models of structure formation predict temperature fluctuations of the order of 10^{-3} , far too large to be consistent with observation. Later, I will mention Peebles' what-you-see-is-what-you-get model [33], also known as PIB for primeval baryon isocurvature fluctuation, which is still viable because the spectrum of perturbations decreases rapidly with scale so that the perturbations that give rise to CBR fluctuations are small (which is no mean feat). Historically, it was fortunate that one started with a low- Ω_0 , baryon-dominated Universe: the theoretical predictions for the CBR fluctuations were sufficiently favorable that experimentalists were stirred

to try to measure them—and then, slowly, theorists lowered their predictions. Had the theoretical expectations begun at 10^{-5} , experimentalists might have been too discouraged to even try!

1.3.3 An initial data problem

With the COBE DMR detection in hand we can praise the success of the gravitational instability scenario; however, the details now remain to be filled in. The structure formation problem is now one of initial data, namely

1. The quantity and composition of matter in the Universe, Ω_0 , Ω_B , and Ω_{other} .
2. The spectrum of initial density perturbations: for the purist, $(\delta\rho/\rho)_{\text{HOR}}$, or for the simulator, the Fourier amplitudes at the epoch of matter-radiation equality.

In a statistical sense, these initial data provide the “blueprint” for the formation of structure.

The initial data are the challenge and the opportunity. Although the gravitational instability picture has been around since the discovery of the CBR itself, the lack of specificity in initial data has impeded progress. With the advent of the study of the earliest history of the Universe a new door was opened. We now have several well motivated early-Universe blueprints: Inflation-produced density perturbations and nonbaryonic dark matter; cosmic-string produced perturbations and nonbaryonic dark matter [34]; texture produced density perturbations and nonbaryonic dark matter [35], and one “conventional model,” a baryon-dominated Universe with isocurvature fluctuations³ [33]. Structure formation provides the opportunity to probe the earliest history of the Universe. I will focus on the cold dark matter “family of models,” which are motivated by inflation. Already the flood of data has all but eliminated the conventional model; the texture and cosmic-string models face severe problems with CBR anisotropy—and who knows, even the cold dark matter models may be eliminated.

2 INFLATIONARY THEORY

2.1 Generalities

As successful as the big-bang cosmology it suffers from a dilemma involving initial data. Extrapolating back, one finds that the Universe apparently began from a very

³Isocurvature baryon-number fluctuations correspond at early times to fluctuations in the local baryon number but not the energy density. At late times, when the Universe is matter dominated, they become fluctuations in the mass density of a comparable amplitude.

special state: A slightly inhomogeneous and very flat Robertson-Walker spacetime. Collins and Hawking showed that the set of initial data that evolve to a spacetime that is as smooth and flat as ours is today of measure zero [36]. (In the context of simple grand unified theories, the hot big bang suffers from another serious problem: the extreme overproduction of superheavy magnetic monopoles; in fact, it was an attempt to solve the monopole problem which led Guth to inflation.)

The cosmological appeal of inflation is its ability to lessen the dependence of the present state of the Universe upon the initial state. Two elements are essential to doing this: (1) accelerated (“superluminal”) expansion and the concomitant tremendous growth of the scale factor; and (2) massive entropy production [38]. Together, these two features allow a small, smooth subhorizon-sized patch of the early Universe to grow to a large enough size and contain enough heat (entropy in excess of 10^{88}) to easily encompass our present Hubble volume. Provided that the region was originally small compared to the curvature radius of the Universe it would appear flat then and today (just as any small portion of the surface of a sphere appears flat).

While there is presently no standard model of inflation—just as there is no standard model for physics at these energies (typically 10^{15} GeV or so)—viable models have much in common. They are based upon well posed, albeit highly speculative, microphysics involving the classical evolution of a scalar field. The superluminal expansion is driven by the potential energy (“vacuum energy”) that arises when the scalar field is displaced from its potential-energy minimum, which results in nearly exponential expansion. Provided the potential is flat, during the time it takes for the field to roll to the minimum of its potential the Universe undergoes many e-foldings of expansion (more than around 60 or so are required to realize the beneficial features of inflation). As the scalar field nears the minimum, the vacuum energy has been converted to coherent oscillations of the scalar field, which correspond to nonrelativistic scalar-field particles. The eventual decay of these particles into lighter particles and their thermalization results in the “reheating” of the Universe and accounts for all the heat in the Universe today (the entropy production event).

Superluminal expansion and the tremendous growth of the scale factor (by a factor greater than that since the end of inflation) allow quantum fluctuations on very small scales ($\lesssim 10^{-23}$ cm) to be stretched to astrophysical scales ($\gtrsim 10^{25}$ cm). Quantum fluctuations in the scalar field responsible for inflation ultimately lead to an almost scale-invariant spectrum of density perturbations [39], and quantum fluctuations in the metric itself lead to an almost scale-invariant spectrum of gravity-waves [40]. Scale invariance for density perturbations means scale-independent fluctuations in the gravitational potential (equivalently, density perturbations of different wavelength cross the horizon with the same amplitude); scale invariance for gravity waves means that gravity waves of all wavelengths cross the horizon with the same amplitude. Because of subsequent evolution, neither the scalar nor the tensor perturbations are scale invariant today.

2.2 Metaphysical implications

Inflation alleviates the “specialness” problem greatly, but does not eliminate all dependence upon the initial state [41]. All open FRW models will inflate and become flat; however, many closed FRW models will recollapse before they can inflate. If one imagines the most general initial spacetime as being comprised of negatively and positively curved FRW (or Bianchi) models that are stitched together, the failure of the positively curved regions to inflate is of little consequence: because of exponential expansion during inflation the negatively curved regions will occupy most of the space today. Nor does inflation solve the smoothness problem forever; it just postpones the problem into the exponentially distant future: We will be able to see outside our smooth inflationary patch and Ω will start to deviate significantly from unity at a time $t \sim t_0 \exp[3(N - N_{\min})]$, where N is the actual number of e-foldings of inflation and $N_{\min} \sim 60$ is the minimum required to solve the horizon/flatness problems.

Linde has emphasized that inflation has changed our view of the Universe in a very fundamental way [42]. While cosmologists have long used the Copernican principle to argue that the Universe must be smooth because of the smoothness of our Hubble volume, in the post-inflation view, our Hubble volume is smooth because it is a small part of a region that underwent inflation. On the largest scales the structure of the Universe is likely to be very rich: Different regions may have undergone different amounts of inflation, may have different laws of physics because they evolved into different vacuum states (of equivalent energy), and may even have different numbers of spatial dimensions. Since it is likely that most of the volume of the Universe is still undergoing inflation and that inflationary patches are being constantly produced (eternal inflation), the age of the Universe is a meaningless concept and our expansion age merely measures the time back to the end of our inflationary event!

2.3 Models

In Guth’s seminal paper [43] he introduced the idea of inflation, sung its praises, and showed that the model that he based the idea upon did not work! Thanks to very important contributions by Linde [44] and Albrecht and Steinhardt [45] that was quickly remedied, and today there are many viable models of inflation. That of course is both good news and bad news; it means that there is no standard model of inflation. Again, the absence of a standard model of inflation should be viewed in the light of our general ignorance about fundamental physics at these energies.

Many different approaches have taken in constructing particle-physics models for inflation. Some have focussed on very simple scalar potentials, e.g., $V(\phi) = \lambda\phi^4$ or $= m^2\phi^2/2$, without regard to connecting the model to any underlying theory [46, 47]. Others have proposed more complicated models that attempt to make contact with speculations about physics at very high energies, e.g., grand unification [48], supersymmetry [49, 50, 51], preonic physics [52], or supergravity [53]. Several authors have attempted to link inflation with superstring theory [54] or “generic predictions”

of superstring theory such as pseudo-Nambu-Goldstone boson fields [55]. While the scale of the vacuum energy that drives inflation is typically of order $(10^{15} \text{ GeV})^4$, a model of inflation at the electroweak scale, vacuum energy $\approx (1 \text{ TeV})^4$, has been proposed [56]. There are also models in which there are multiple epochs of inflation [57].

In all of the models above gravity is described by general relativity. A qualitatively different approach is to consider inflation in the context of alternative theories of gravity. (After all, inflation probably involves physics at energy scales not too different from the Planck scale and the effective theory of gravity at these energies could well be very different from general relativity; in fact, there are some indications from superstring theory that gravity in these circumstances might be described by a Brans-Dicke like theory.) Perhaps the most successful of these models is first-order inflation [58, 59]. First-order inflation returns to Guth’s original idea of a strongly first-order phase transition; in the context of general relativity Guth’s model failed because the phase transition, if inflationary, never completed. In theories where the effective strength of gravity evolves, like Brans-Dicke theory, the weakening of gravity during inflation allows the transition to complete. In other models based upon nonstandard gravitation theory, the scalar field responsible for inflation is itself related to the size of additional spatial dimensions, and inflation then also explains why our three spatial dimensions are so big, while the other spatial dimensions are so small.

All models of inflation have one feature in common: the scalar field responsible for inflation has a very flat potential-energy curve and is very weakly coupled. This typically leads to a very small dimensionless number, usually a dimensionless coupling of the order of 10^{-14} . Such a small number, like other small numbers in physics (e.g., the ratio of the weak to Planck scales $\approx 10^{-17}$ or the ratio of the mass of the electron to the W/Z boson masses $\approx 10^{-5}$), runs counter to one’s belief that a truly fundamental theory should have no tiny parameters, and cries out for an explanation. At the very least, this small number must be stabilized against quantum corrections—which it is in all of the previously mentioned models.⁴ In some models, the small number in the inflationary potential is related to other small numbers in particle physics: for example, the ratio of the electron mass to the weak scale or the ratio of the unification scale to the Planck scale. Explaining the origin of the small number that seems to be associated with inflation is both a challenge and an opportunity.

Because of the growing base of observations that bear on inflation, another approach to model building is emerging: the use of observations to constrain the underlying inflationary potential. I will return to “reconstructing” the inflationary potential from data later. Before going on, I want to emphasize that while there are many varieties of inflation, there are robust predictions which are crucial to sharply testing

⁴It is sometimes stated that inflation is unnatural because of the small coupling of the scalar field responsible for inflation; while the small coupling certainly begs explanation, these inflationary models are not unnatural in the rigorous technical sense as the small number is stable against quantum fluctuations.

inflation.

2.4 Three robust predictions

Inflation makes three robust⁵ predictions:

1. **Flat universe.** Because solving the “horizon” problem (large-scale smoothness in spite of small particle horizons at early times) and solving the “flatness” problem (maintaining Ω very close to unity until the present epoch) are linked geometrically [37, 38], this is the most robust prediction of inflation. Said another way, it is the prediction that most inflationists would be least willing to give up. (Even so, models of inflation have been constructed where the amount of inflation is tuned just to give Ω_0 less than one today [60].) Through the Friedmann equation for the scale factor, flat implies that the total energy density (matter, radiation, vacuum energy, ...) is equal to the critical density.
2. **Nearly scale-invariant spectrum of gaussian density perturbations.** Essentially all inflation models predict a nearly, but not exactly, scale-invariant spectrum of gaussian density perturbations [47]. Described in terms of a power spectrum, $P(k) \equiv \langle |\delta_k|^2 \rangle = Ak^n$, where δ_k is the Fourier transform of the primeval density perturbations, and the spectral index $n \approx 1$ (the scale-invariant limit is $n = 1$). The inflationary prediction is statistical: the δ_k are drawn from a gaussian distribution whose variance is $|\delta_k|^2$. The overall amplitude A is very model dependent. Density perturbations give rise to CBR anisotropy as well as seeding structure formation. Requiring that the density perturbations are consistent with the observed level of anisotropy of the CBR (and large enough to produce the observed structure formation) is the most severe constraint on inflationary models and leads to the small dimensionless number that all inflationary models have.
3. **Nearly scale-invariant spectrum of gravitational waves.** These gravitational waves have wavelengths from $\mathcal{O}(1\text{ km})$ to the size of the present Hubble radius and beyond. Described in terms of a power spectrum for the dimensionless gravity-wave amplitude at early times, $P_T(k) \equiv \langle |h_k|^2 \rangle = A_T k^{n_T-3}$, where the spectral index $n_T \approx 0$ (the scale-invariant limit is $n_T = 0$). As before, the power spectrum specifies the variance of the Fourier components. Once again, the overall amplitude A_T is model dependent (varying as the value of the inflationary vacuum energy). Unlike density perturbations, which are required to initiate structure formation, there is no cosmological lower bound to the amplitude of the gravity-wave perturbations. Tensor perturbations also give rise to CBR anisotropy; requiring that they do not lead to excessive anisotropy

⁵Because theorists are so clever, it is not possible nor prudent to use the word immutable. Models that violate any or all of these “robust predications” can and have been constructed.

implies that the energy density that drove inflation must be less than about $(10^{16} \text{ GeV})^4$. This indicates that if inflation took place, it did so at an energy well below the Planck scale.⁶

There are other interesting consequences of inflation that are less generic. For example, in models of first-order inflation, in which reheating occurs through the nucleation and collision of vacuum bubbles, there is an additional, larger amplitude, but narrow-band, spectrum of gravitational waves ($\Omega_{\text{GW}} h^2 \sim 10^{-6}$) [61]. In other models large-scale primeval magnetic fields of interesting size are seeded during inflation [62].

3 Inflation: The Details

In this Section I discuss how to analyze an inflationary model, given the scalar potential. In two sections hence I will work through a number of examples. The focus will be on the metric perturbations—density fluctuations [39] and gravity waves [40]—that arise due to quantum fluctuations, and the CBR temperature anisotropies that result from them.⁷ Perturbations on all astrophysically interesting scales, say 1 Mpc to 10^4 Mpc, are produced during an interval of about 8 e-folds around 50 e-folds before the end of inflation, when these scales crossed outside the horizon during inflation. I will show how the density perturbations and gravity waves can be related to three features of the inflationary potential: its value V_{50} , its steepness $x_{50} \equiv (m_{\text{Pl}} V'/V)_{50}$, and the change in its steepness x'_{50} , evaluated in the region of the potential where the scalar field was about 50 e-folds before the end of inflation. In principle, cosmological observations, most importantly CBR anisotropy, can be used to determine the characteristics of the density perturbations and gravitational waves and thereby V_{50} , x_{50} , and x'_{50} .

All viable models of inflation are of the slow-rollover variety, or can be recast as such [65]. In slow-rollover inflation a scalar field that is initially displaced from the minimum of its potential rolls slowly to that minimum, and as it does the cosmic-scale factor grows very rapidly. Once the scalar field reaches the minimum of the potential it oscillates about it, so that the large potential energy has been converted into coherent scalar-field oscillations, corresponding to a condensate of nonrelativistic scalar particles. The eventual decay of these particles into lighter particle states and their subsequent thermalization lead to the reheating of the Universe to a temperature $T_{\text{RH}} \simeq \sqrt{\Gamma m_{\text{Pl}}}$, where Γ is the decay width of the scalar particle [64, 65]. Here, I

⁶To be more precise, the part of inflation that led to perturbations on scales within the present horizon involved subPlanckian energy densities. In some models of inflation, the earliest stages, which do not influence scales that we are privy to, involve energies as large as the Planck scale.

⁷Isocurvature perturbations can arise due to quantum fluctuations in other massless fields, e.g., the axion field, if it exists [63].

will focus on the classical evolution of the inflaton field during the slow-roll phase and the small quantum fluctuations in the inflaton field which give rise to density perturbations and those in the metric which give rise to gravity waves.

To begin, let us assume that the scalar field driving inflation is minimally coupled so that its stress-energy tensor takes the canonical form,

$$T_{\mu\nu} = \partial_\mu\phi\partial_\nu\phi - \mathcal{L}g_{\mu\nu}; \quad (23)$$

where the Lagrangian density of the scalar field $\mathcal{L} = \frac{1}{2}\partial_\mu\phi\partial^\mu\phi - V(\phi)$. If we make the usual assumption that the scalar field ϕ is spatially homogeneous, or at least so over a Hubble radius, the stress-energy tensor takes the perfect-fluid form with energy density, $\rho = \frac{1}{2}\dot{\phi}^2 + V(\phi)$, and isotropic pressure, $p = \frac{1}{2}\dot{\phi}^2 - V(\phi)$. The classical equations of motion for ϕ can be obtained from the first law of thermodynamics, $d(R^3\rho) = -pdR^3$, or by taking the four-divergence of $T^{\mu\nu}$:

$$\ddot{\phi} + 3H\dot{\phi} + V'(\phi) = 0; \quad (24)$$

the $\Gamma\dot{\phi}$ term responsible for reheating has been omitted since we shall only be interested in the slow-rollover phase. In addition, there is the Friedmann equation, which governs the expansion of the Universe,

$$H^2 = \frac{8\pi}{3m_{\text{Pl}}^2} \left(V(\phi) + \frac{1}{2}\dot{\phi}^2 \right) \simeq \frac{8\pi V(\phi)}{3m_{\text{Pl}}^2}; \quad (25)$$

where we assume that the contribution of all other forms of energy density, e.g., radiation and kinetic energy of the scalar field, and the curvature term (k/R^2) are negligible. The justification for discussing inflation in the context of a flat FRW model with a homogeneous scalar field driving inflation were discussed earlier (and at greater length in Ref. [66]); including the ϕ kinetic term increases the righthand side of Eq. (25) by a factor of $(1 + x^2/48\pi)$, a small correction for viable models.

In the next Section I will be more precise about the amplitude of density perturbations and gravitational waves; for now, let me briefly discuss how these perturbations arise and give their characteristic amplitudes. The metric perturbations produced in inflationary models are very nearly “scale invariant,” a particularly simple spectrum which was first discussed by Harrison and Zel’dovich [67], and arise due to quantum fluctuations. In deSitter space all massless scalar fields experience quantum fluctuations of amplitude $H/2\pi$. The graviton is massless and can be described by two massless scalar fields, $h_{+,\times} = \sqrt{16\pi G}\phi_{+,\times}$ (+ and \times are the two polarization states). The inflaton by virtue of its flat potential is for all practical purposes massless.

Fluctuations in the inflaton field lead to density fluctuations because of its scalar potential, $\delta\rho \sim HV'$; as a given mode crosses outside the horizon, the density perturbation on that scale becomes a classical metric perturbation. While outside the horizon, the description of the evolution of a density perturbation is beset with subtleties associated with the gauge freedom in general relativity; there is, however, a simple gauge-invariant quantity, $\zeta \simeq \delta\rho/(\rho + p)$, which remains constant outside the

horizon. By equating the value of ζ at postinflation horizon crossing with its value as the scale crosses outside the horizon it follows that $(\delta\rho/\rho)_{\text{HOR}} \sim HV'/\dot{\phi}^2$ (note: $\rho + p = \dot{\phi}^2$); see Fig. 7.

The evolution of a gravity-wave perturbation is even simpler; it obeys the massless Klein-Gordon equation

$$\ddot{h}_k^i + 3H\dot{h}_k^i + k^2 h_k^i / R^2 = 0; \quad (26)$$

where k is the wavenumber of the mode and $i = +, \times$. For superhorizon sized modes, $k \lesssim RH$, the solution is simple: $h_k^i = \text{const.}$ Like their density perturbation counterparts, gravity-wave perturbations become classical metric perturbations as they cross outside the horizon; they are characterized by an amplitude $h_k^i \simeq \sqrt{16\pi G}(H/2\pi) \sim H/m_{\text{Pl}}$. At postinflation horizon crossing their amplitude is unchanged.

Finally, let me write the horizon-crossing amplitudes of the scalar and tensor metric perturbations in terms of the inflationary potential,

$$(\delta\rho/\rho)_{\text{HOR},\lambda} = c_S \left(\frac{V^{3/2}}{m_{\text{Pl}}^3 V'} \right)_1; \quad (27)$$

$$h_{\text{HOR},\lambda} = c_T \left(\frac{V^{1/2}}{m_{\text{Pl}}^2} \right)_1; \quad (28)$$

where $(\delta\rho/\rho)_{\text{HOR},\lambda}$ is the amplitude of the density perturbation on the scale λ when it crosses the Hubble radius during the post-inflation epoch, $h_{\text{HOR},\lambda}$ is the dimensionless amplitude of the gravitational wave perturbation on the scale λ when it crosses the Hubble radius, and c_S, c_T are numerical constants of order unity. Subscript 1 indicates that the quantity involving the scalar potential is to be evaluated when the scale in question crossed outside the horizon during the inflationary era. The metric perturbations produced by inflation are characterized by almost scale-invariant horizon-crossing amplitudes; the slight deviations from scale invariance result from the variation of V and V' during inflation which enter through the dependence upon t_1 . [In Eq. (27) I got ahead of myself and used the slow-roll approximation (see below) to rewrite the expression, $(\delta\rho/\rho)_{\text{HOR},\lambda} \simeq HV'/\dot{\phi}$, in terms of the potential only.]

Eqs. (24-27) are the fundamental equations that govern inflation and the production of metric perturbations. It proves very useful to recast these equations using the scalar field as the independent variable; we then express the scalar and tensor perturbations in terms of the value of the potential, its steepness, and the rate of change of its steepness when the interesting scales crossed outside the Hubble radius during inflation, about 50 e-folds in scale factor before the end of inflation, defined by

$$V_{50} \equiv V(\phi_{50}); \quad x_{50} \equiv \frac{m_{\text{Pl}} V'(\phi_{50})}{V(\phi_{50})}; \quad x'_{50} = \frac{m_{\text{Pl}} V''(\phi_{50})}{V(\phi_{50})} - \frac{m_{\text{Pl}} [V'(\phi_{50})]^2}{V^2(\phi_{50})}.$$

To evaluate these three quantities 50 e-folds before the end of inflation we must find the value of the scalar field at this time. During the inflationary phase the $\ddot{\phi}$ term is negligible (the motion of ϕ is friction dominated), and Eq. (24) becomes

$$\dot{\phi} \simeq \frac{-V'(\phi)}{3H}; \quad (29)$$

this is known as the slow-roll approximation [47]. While the slow-roll approximation is almost universally applicable, there are models where the slow-roll approximation cannot be used; e.g., a potential where during the crucial 8 e-folds the scalar field rolls uphill, “powered” by the velocity it had when it hit the incline.

The conditions that must be satisfied in order that $\ddot{\phi}$ be negligible are:

$$|V''| < 9H^2 \simeq 24\pi V/m_{\text{Pl}}^2; \quad (30)$$

$$|x| \equiv |V'm_{\text{Pl}}/V| < \sqrt{48\pi}. \quad (31)$$

The end of the slow roll occurs when either or both of these inequalities are saturated, at a value of ϕ denoted by ϕ_{end} . Since $H \equiv \dot{R}/R$, or $Hdt = d \ln R$, it follows that

$$d \ln R = \frac{8\pi}{m_{\text{Pl}}^2} \frac{V(\phi)d\phi}{-V'(\phi)} = -\frac{8\pi d\phi}{m_{\text{Pl}} x}. \quad (32)$$

Now express the cosmic-scale factor in terms of its value at the end of inflation, R_{end} , and the number of e-foldings before the end of inflation, $N(\phi)$,

$$R = \exp[-N(\phi)] R_{\text{end}}.$$

The quantity $N(\phi)$ is a time-like variable whose value at the end of inflation is zero and whose evolution is governed by

$$\frac{dN}{d\phi} = \frac{8\pi}{m_{\text{Pl}} x}. \quad (33)$$

Using Eq. (33) we can compute the value of the scalar field 50 e-folds before the end of inflation ($\equiv \phi_{50}$); the values of V_{50} , x_{50} , and x'_{50} follow directly.

As ϕ rolls down its potential during inflation its energy density decreases, and so the growth in the scale factor is not exponential. By using the fact that the stress-energy of the scalar field takes the perfect-fluid form, we can solve for evolution of the cosmic-scale factor. Recall, for the equation of state $p = \gamma\rho$, the scale factor grows as $R \propto t^q$, where $q = 2/3(1 + \gamma)$. Here,

$$\gamma = \frac{\frac{1}{2}\dot{\phi}^2 - V}{\frac{1}{2}\dot{\phi}^2 + V} = \frac{x^2 - 48\pi}{x^2 + 48\pi}; \quad (34)$$

$$q = \frac{1}{3} + \frac{16\pi}{x^2}. \quad (35)$$

Since the steepness of the potential can change during inflation, γ is not in general constant; the power-law index q is more precisely the logarithmic rate of the change of the logarithm of the scale factor, $q = d \ln R / d \ln t$.

When the steepness parameter is small, corresponding to a very flat potential, γ is close to -1 and the scale factor grows as a very large power of time. To solve the horizon problem the expansion must be “superluminal” ($\dot{R} > 0$), corresponding to $q > 1$, which requires that $x^2 < 24\pi$. Since $\frac{1}{2}\dot{\phi}^2/V = x^2/48\pi$, this implies that $\frac{1}{2}\dot{\phi}^2/V(\phi) < \frac{1}{2}$, justifying neglect of the scalar-field kinetic energy in computing the expansion rate for all but the steepest potentials. (In fact there are much stronger constraints; the COBE DMR data imply that $n \gtrsim 0.5$, which restricts $x_{50}^2 \lesssim 4\pi$, $\frac{1}{2}\dot{\phi}^2/V \lesssim \frac{1}{12}$, and $q \gtrsim 4$.)

Next, let us relate the size of a given scale to when that scale crosses outside the Hubble radius during inflation, specified by $N_1(\lambda)$, the number of e-folds before the end of inflation. The physical size of a perturbation is related to its comoving size, $\lambda_{\text{phys}} = R\lambda$; with the usual convention, $R_{\text{today}} = 1$, the comoving size is the physical size today. When the scale λ crosses outside the Hubble radius $R_1\lambda = H_1^{-1}$. We then assume that: (1) at the end of inflation the energy density is $\mathcal{M}^4 \simeq V(\phi_{\text{end}})$; (2) inflation is followed by a period where the energy density of the Universe is dominated by coherent scalar-field oscillations which decrease as R^{-3} ; and (3) when value of the scale factor is R_{RH} the Universe reheats to a temperature $T_{\text{RH}} \simeq \sqrt{m_{\text{Pl}}\Gamma}$ and expands adiabatically thereafter. The “matching equation” that relates λ and $N_1(\lambda)$ is:

$$\lambda = \frac{R_{\text{today}}}{R_1} H_1^{-1} = \frac{R_{\text{today}}}{R_{\text{RH}}} \frac{R_{\text{RH}}}{R_{\text{end}}} \frac{R_{\text{end}}}{R_1} H_1^{-1}. \quad (36)$$

Adiabatic expansion since reheating implies $R_{\text{today}}/R_{\text{RH}} \simeq T_{\text{RH}}/2.73 \text{ K}$; and the decay of the coherent scalar-field oscillations implies $(R_{\text{RH}}/R_{\text{end}})^3 = (\mathcal{M}/T_{\text{RH}})^4$. If we define $\bar{q} = \ln(R_{\text{end}}/R_1)/\ln(t_{\text{end}}/t_1)$, the mean power-law index, it follows that $(R_{\text{end}}/R_1)H_1^{-1} = \exp[N_1(\bar{q} - 1)/\bar{q}]H_{\text{end}}^{-1}$, and Eq. (36) becomes

$$N_1(\lambda) = \frac{\bar{q}}{\bar{q} - 1} \left[48 + \ln \lambda_{\text{Mpc}} + \frac{2}{3} \ln(\mathcal{M}/10^{14} \text{ GeV}) + \frac{1}{3} \ln(T_{\text{RH}}/10^{14} \text{ GeV}) \right]; \quad (37)$$

In the case of perfect reheating, which probably only applies to first-order inflation, $T_{\text{RH}} \simeq \mathcal{M}$.

The scales of astrophysical interest today range roughly from that of galaxy size, $\lambda \sim \text{Mpc}$, to the present Hubble scale, $H_0^{-1} \sim 10^4 \text{ Mpc}$; up to the logarithmic corrections these scales crossed outside the horizon between about $N_1(\lambda) \sim 48$ and $N_1(\lambda) \simeq 56$ e-folds before the end of inflation. *That is, the interval of inflation that determines its all observable consequences covers only about 8 e-folds.*

Except in the case of strict power-law inflation q varies during inflation; this means that the $(R_{\text{end}}/R_1)H_1^{-1}$ factor in Eq. (36) cannot be written in closed form. Taking account of this, the matching equation becomes a differential equation,

$$\frac{d \ln \lambda_{\text{Mpc}}}{d N_1} = \frac{q(N_1) - 1}{q(N_1)}; \quad (38)$$

subject to the “boundary condition:”

$$\ln \lambda_{\text{Mpc}} = -48 - \frac{4}{3} \ln(\mathcal{M}/10^{14} \text{ GeV}) + \frac{1}{3} \ln(T_{\text{RH}}/10^{14} \text{ GeV})$$

for $N_1 = 0$, the matching relation for the mode that crossed outside the Hubble radius at the end of inflation. Equation (38) allows one to obtain the precise expression for when a given scale crossed outside the Hubble radius during inflation. To actually solve this equation, one would need to supplement it with the expressions $dN/d\phi = 8\pi/m_{\text{Pl}}x$ and $q = 16\pi/x^2$. For our purposes we need only know: (1) The scales of astrophysical interest correspond to $N_1 \sim “50 \pm 4,”$ where for definiteness we will throughout take this to be an equality sign. (2) The expansion of Eq. (38) about $N_1 = 50$,

$$\Delta N_1(\lambda) = \left(\frac{q_{50} - 1}{q_{50}} \right) \Delta \ln \lambda_{\text{Mpc}}; \quad (39)$$

which, with the aid of Eq. (33), implies that

$$\Delta \phi = \left(\frac{q_{50} - 1}{q_{50}} \right) \frac{x_{50}}{8\pi} \Delta \lambda_{\text{Mpc}}. \quad (40)$$

We are now ready to express the perturbations in terms of V_{50} , x_{50} , and x'_{50} . First, we must solve for the value of ϕ , 50 e-folds before the end of inflation. To do so we use Eq. (33),

$$N(\phi_{50}) = 50 = \frac{8\pi}{m_{\text{Pl}}^2} \int_{\phi_{\text{end}}}^{\phi_{50}} \frac{V d\phi}{V'}. \quad (41)$$

Next, with the help of Eq. (40) we expand the potential V and its steepness x about ϕ_{50} :

$$V \simeq V_{50} + V'_{50}(\phi - \phi_{50}) = V_{50} \left[1 + \frac{x_{50}^2}{8\pi} \left(\frac{q_{50}}{q_{50} - 1} \right) \Delta \ln \lambda_{\text{Mpc}} \right]; \quad (42)$$

$$x \simeq x_{50} + x'_{50}(\phi - \phi_{50}) = x_{50} \left[1 + \frac{m_{\text{Pl}} x'_{50}}{8\pi} \left(\frac{q_{50}}{q_{50} - 1} \right) \Delta \ln \lambda_{\text{Mpc}} \right]; \quad (43)$$

of course these expansions only make sense for potentials that are smooth. We note that additional terms in either expansion are $\mathcal{O}(\alpha_i^2)$ and beyond the accuracy we are seeking.

Now recall the equations for the amplitude of the scalar and tensor perturbations,

$$(\delta\rho/\rho)_{\text{HOR},\lambda} = c_S \left(\frac{V^{1/2}}{m_{\text{Pl}}^2 x} \right)_1; \quad (44)$$

$$h_{\text{HOR},\lambda} = c_T \left(\frac{V^{1/2}}{m_{\text{Pl}}^2} \right)_1; \quad (45)$$

where subscript 1 means that the quantities are to be evaluated where the scale λ crossed outside the Hubble radius, $N_1(\lambda)$ e-folds before the end of inflation. The

origin of any deviation from scale invariance is clear: For tensor perturbations it arises due to the variation of the potential; and for scalar perturbations it arises due to the variation of both the potential and its steepness.

Using Eqs. (39-44) it is now simple to calculate the power-law exponents α_S and α_T that quantify the deviations from scale invariance,

$$\alpha_T = \frac{x_{50}^2}{16\pi} \frac{q_{50}}{q_{50} - 1} \simeq \frac{x_{50}^2}{16\pi}; \quad (46)$$

$$\alpha_S = \alpha_T - \frac{m_{\text{Pl}} x'_{50}}{8\pi} \frac{q_{50}}{q_{50} - 1} \simeq \frac{x_{50}^2}{16\pi} - \frac{m_{\text{Pl}} x'_{50}}{8\pi}; \quad (47)$$

where

$$q_{50} = \frac{1}{3} + \frac{16\pi}{x_{50}^2} \simeq \frac{16\pi}{x_{50}^2}; \quad (48)$$

$$h_{\text{HOR},\lambda} = c_T \left(\frac{V_{50}^{1/2}}{m_{\text{Pl}}^2} \right) \lambda_{\text{Mpc}}^{\alpha_T}; \quad (49)$$

$$(\delta\rho/\rho)_{\text{HOR},\lambda} = c_S \left(\frac{V_{50}^{1/2}}{x_{50} m_{\text{Pl}}^2} \right) \lambda_{\text{Mpc}}^{\alpha_S}. \quad (50)$$

The spectral indices α_i are defined as, $\alpha_S = [d \ln(\delta\rho/\rho)_{\text{HOR},\lambda} / d \ln \lambda_{\text{Mpc}}]_{50}$ and $\alpha_T = [d \ln h_{\text{HOR},\lambda} / d \ln \lambda_{\text{Mpc}}]_{50}$, and in general vary slowly with scale. Note too that the deviations from scale invariance, quantified by α_S and α_T , are of the order of x_{50}^2 , $m_{\text{Pl}} x'_{50}$. In the expressions above we retained only lowest-order terms in $\mathcal{O}(\alpha_i)$. The next-order contributions to the spectral indices are $\mathcal{O}(\alpha_i^2)$; those to the amplitudes are $\mathcal{O}(\alpha_i)$ and are given two sections hence. The justification for truncating the expansion at lowest order is that the deviations from scale invariance are expected to be small—and are required by astrophysical data to be small.

As I discuss in more detail two sections hence, the more intuitive power-law indices α_S , α_T are related to the indices that are usually used to describe the power spectra of scalar and tensor perturbations, $P_S(k) \equiv |\delta_k|^2 = A k^n$ and $P_T(k) \equiv |h_k|^2 = A_T k^{n_T}$,

$$n = 1 - 2\alpha_S = 1 - \frac{x_{50}^2}{8\pi} + \frac{m_{\text{Pl}} x'_{50}}{4\pi}; \quad (51)$$

$$n_T = -2\alpha_T = -\frac{x_{50}^2}{8\pi}. \quad (52)$$

$$(53)$$

CBR temperature fluctuations on large-angular scales ($\theta \gtrsim 1^\circ$) due to metric perturbations arise through the Sachs-Wolfe effect; very roughly, the temperature fluctuation on a given angular scale θ is related to the metric fluctuation on the length scale that subtends that angle at last scattering, $\lambda \sim 100 h^{-1} \text{Mpc}(\theta/\text{deg})$,

$$\left(\frac{\delta T}{T} \right)_\theta \sim \left(\frac{\delta\rho}{\rho} \right)_{\text{HOR},\lambda}; \quad (54)$$

$$\left(\frac{\delta T}{T}\right)_\theta \sim h_{\text{HOR},\lambda}; \quad (55)$$

where the scalar and tensor contributions to the CBR temperature anisotropy on a given scale add in quadrature. Let me be more specific about the amplitude of the quadrupole CBR anisotropy. For small α_S , α_T the contributions of each to the quadrupole CBR temperature anisotropy:

$$\left(\frac{\Delta T}{T_0}\right)_{Q-S}^2 \approx \frac{32\pi}{45} \frac{V_{50}}{m_{\text{Pl}}^4 x_{50}^2}; \quad (56)$$

$$\left(\frac{\Delta T}{T_0}\right)_{Q-T}^2 \approx 0.61 \frac{V_{50}}{m_{\text{Pl}}^4}; \quad (57)$$

$$\frac{T}{S} \equiv \frac{(\Delta T/T_0)_{Q-T}^2}{(\Delta T/T_0)_{Q-S}^2} \approx 0.28 x_{50}^2; \quad (58)$$

where expressions have been evaluated to lowest order in x_{50}^2 and $m_{\text{Pl}} x'_{50}$. In terms of the spherical-harmonic expansion of the CBR temperature anisotropy, the square of the quadrupole anisotropy is defined to be $\sum_{m=-2}^{m=2} |a_{2m}|^2 / 4\pi$.

So what are these quantities precisely? Inflation makes statistical predictions. The underlying density perturbations are gaussian and the expression for $|\delta_k|^2$ is simply the variance of the gaussian distribution for δ_k . Because the predicted multipole amplitudes a_{lm} depend linearly upon δ_k and h_k , the distribution of multipole amplitudes is gaussian, with variance $\equiv \langle |a_{lm}|^2 \rangle$. This underlying variance is comprised of scalar and tensor contributions.

How accurately can one hope to estimate the actual variance of the underlying distribution? If one had an ensemble of observers distributed throughout the Universe who each measured the CBR anisotropy at their position, then one could determine the underlying variance to arbitrary precision by averaging their $|a_{lm}|^2$'s (hence the notation $\langle |a_{lm}|^2 \rangle$ for the underlying variance). However, we are privy to but one CBR sky and for multipole l , only $2l + 1$ multipole amplitudes. Thus, we can only estimate the actual variance with finite precision. This is nothing other than ordinary sampling variance, but is often called “cosmic variance.” The sampling variance of $\langle |a_{lm}|^2 \rangle$ —which is the irreducible uncertainty in measuring $\langle |a_{lm}|^2 \rangle$ —is simply given by $2\langle |a_{lm}|^2 \rangle^2 / (2l + 1)$. The distribution of the measured value of $\langle |a_{lm}|^2 \rangle_{\text{MEAS}}$ is just the χ^2 distribution for $2l + 1$ degrees of freedom.

Before going on, some general remarks [68]. The steepness parameter x_{50}^2 must be less than about 24π to ensure superluminal expansion. For “steep” potentials, the expansion rate is “slow,” i.e., q_{50} closer to unity, the gravity-wave contribution to the quadrupole CBR temperature anisotropy becomes comparable to, or greater than, that of density perturbations, and both scalar and tensor perturbations exhibit significant deviations from scale invariance. For “flat” potentials, i.e., small x_{50} , the expansion rate is “fast,” i.e., $q_{50} \gg 1$, the gravity-wave contribution to the quadrupole CBR temperature anisotropy is much smaller than that of density perturbations, and

the tensor perturbations are scale invariant. Unless the steepness of the potential changes rapidly, i.e., large x'_{50} , the scalar perturbations are also scale invariant.

3.1 Metric perturbations and CBR anisotropy

I was purposefully vague when discussing the amplitudes of the scalar and tensor modes, except when specifying their contributions to the quadrupole CBR temperature anisotropy; in fact, the spectral indices α_S and α_T , together with the scalar and tensor contributions to the CBR quadrupole serve to provide all the information necessary. Here I will fill in more details about the metric perturbations.

The scalar and tensor metric perturbations are expanded in harmonic functions, in the flat Universe predicted by inflation, plane waves,

$$h_{\mu\nu}(\mathbf{x}, t) = \frac{1}{(2\pi)^3} \int d^3k h_{\mathbf{k}}^i(t) \varepsilon_{\mu\nu}^i e^{-i\mathbf{k}\cdot\mathbf{x}}, \quad (59)$$

$$\frac{\delta\rho(\mathbf{x}, t)}{\rho} = \frac{1}{(2\pi)^3} \int d^3k \delta_{\mathbf{k}}(t) e^{-i\mathbf{k}\cdot\mathbf{x}}, \quad (60)$$

where $h_{\mu\nu} = R^{-2}g_{\mu\nu} - \eta_{\mu\nu}$, $\varepsilon_{\mu\nu}^i$ is the polarization tensor for the gravity-wave modes, and $i = +, \times$ are the two polarization states. Everything of interest can be computed in terms of $h_{\mathbf{k}}^i$ and $\delta_{\mathbf{k}}$. For example, the *rms* mass fluctuation in a sphere of radius r is obtained in terms of the window function for a sphere and the power spectrum $P_S(k) \equiv \langle |\delta_{\mathbf{k}}|^2 \rangle$ (see below),

$$\langle (\delta M/M)^2 \rangle_r = \frac{9}{2\pi^2 r^2} \int_0^\infty [j_1(kr)]^2 P_S(k) dk; \quad (61)$$

where $j_1(x)$ is the spherical Bessel function of first order. If $P_S(k)$ is a power law, it follows roughly that $(\delta M/M)^2 \sim k^3 |\delta_{\mathbf{k}}|^2$, evaluated on the scale $k = r^{-1}$. This is what I meant by $(\delta\rho/\rho)_{\text{HOR},\lambda}$: the *rms* mass fluctuation on the scale λ when it crossed inside the horizon. Likewise, by $h_{\text{HOR},\lambda}$ I meant the *rms* strain on the scale λ as it crossed inside the Hubble radius, $(h_{\text{HOR},\lambda})^2 \sim k^3 |h_{\mathbf{k}}^i|^2$.

In the previous discussions I have chosen to specify the metric perturbations for the different Fourier modes when they crossed inside the horizon, rather than at a common time. I did so because scale invariance is made manifest, as the scale independence of the metric perturbations at post-inflation horizon crossing. Recall, in the case of scalar perturbations $(\delta\rho/\rho)_{\text{HOR}}$ is up to a numerical factor the fluctuation in the Newtonian potential, and, by specifying the scalar perturbations at horizon crossing, we avoid the discussion of scalar perturbations on superhorizon scales, which is beset by the subtleties associated with the gauge noninvariance of $\delta_{\mathbf{k}}$.

It is, however, necessary to specify the perturbations at a common time to carry out most calculations; e.g., an N -body simulation of structure formation or the calculation of CBR anisotropy. To do so, one has to take account of the evolution of the perturbations after they enter the horizon. After entering the horizon tensor perturbations behave like gravitons, with $h_{\mathbf{k}}$ decreasing as R^{-1} and the energy density

associated with a given mode, $\rho_k \sim m_{\text{Pl}}^2 k^5 |h_{\mathbf{k}}|^2 / R^2$, decreasing as R^{-4} . The evolution of scalar perturbations is slightly more complicated; modes that enter the horizon while the Universe is still radiation dominated remain essentially constant until the Universe becomes matter dominated (growing only logarithmically); modes that enter the horizon after the Universe becomes matter dominated grow as the scale factor. (The gauge noninvariance of $\delta_{\mathbf{k}}$ is not an important issue for subhorizon size modes. A Newtonian analysis suffices, and there is only one growing mode, corresponding to a density perturbation.)

The method for characterizing the scalar perturbations is by now standard: The spectrum of perturbations is specified at the present epoch (assuming linear growth for all scales); the spectrum at earlier epochs can be obtained by multiplying $\delta_{\mathbf{k}}$ by $R(t)/R_{\text{today}}$. The inflationary metric perturbations are gaussian; thus $\delta_{\mathbf{k}}$ is a gaussian, random variable. Its statistical expectation value is

$$\langle \delta_{\mathbf{k}} \delta_{\mathbf{q}} \rangle = P_S(k) (2\pi)^3 \delta^{(3)}(\mathbf{k} - \mathbf{q}); \quad (62)$$

where the power spectrum today is written as

$$P_S(k) \equiv A k^n T(k)^2; \quad (63)$$

$n = 1 - 2\alpha_S$ ($= 1$ for scale-invariant perturbations), and $T(k)$ is the “transfer function” which encodes the information about the post-horizon crossing evolution of each mode and depends upon the matter content of the Universe, e.g., baryons plus cold dark matter, baryons plus hot dark matter, baryons plus hot and cold dark matter, and so on. The transfer function is defined so that $T(k) \rightarrow 1$ for $k \rightarrow 0$ (long-wavelength perturbations); an analytic approximation to the cold dark matter transfer function is given by [69]

$$T(k) = \frac{\ln(1 + 2.34q)/2.34q}{[1 + (3.89q) + (16.1q)^2 + (5.46q)^3 + (6.71q)^4]^{1/4}}; \quad (64)$$

where $q = k/(\Omega_0 h^2 \text{Mpc}^{-1})$. Inflationary power spectra for different dark matter possibilities are shown in Fig. 9.

The overall normalization factor

$$A = \frac{1024\pi^3}{75H_0^4} \frac{V_{50}}{m_{\text{Pl}}^4 x_{50}^2} \frac{[1 + \frac{7}{6}n_T - \frac{1}{3}(n-1)] \left\{ \Gamma[\frac{3}{2} - \frac{1}{2}(n-1)] \right\}^2}{2^{n-1} [\Gamma(\frac{3}{2})]^2} k_{50}^{1-n}; \quad (65)$$

where the $\mathcal{O}(\alpha_i)$ correction to A has been included [70]. The quantity $n_T = -2\alpha_T = -x_{50}^2/8\pi$, $n-1 = -2\alpha_S = n_T + x_{50}'/4\pi$, k_{50} is the comoving wavenumber of the scale that crossed outside the horizon 50 e-folds before the end of inflation. All the formulas below simplify if this scale corresponds to the present horizon scale, specifically, $k_{50} = H_0/2$. [Eq. (65) can be simplified by expanding $\Gamma(\frac{3}{2}+x) = \Gamma(3/2)[1+x(2-2\ln 2-\gamma)]$, valid for $|x| \ll 1$; $\gamma \simeq 0.577$ is Euler’s constant.]

Figure 7: Comparison of the cold dark matter perturbation spectrum with CBR anisotropy measurements (boxes) and the distribution of galaxies today (triangles). Wavenumber k is related to length scale, $k = 2\pi/\lambda$; error flags are not shown for the galaxy distribution. The curve labeled MDM is hot + cold dark matter (“5 eV” worth of neutrinos); the other two curves are cold dark matter models with Hubble constants of $50 \text{ km s}^{-1} \text{ Mpc}$ (labeled CDM) and $35 \text{ km s}^{-1} \text{ Mpc}$. (Figure courtesy of M. White.)

From this expression it is simple to compute the Sachs-Wolfe contribution of scalar perturbations to the CBR temperature anisotropy; on angular scales much greater than about 1° (corresponding to multipoles $l \ll 100$) it is the dominant contribution. It is useful to expand the CBR temperature on the sky in spherical harmonics,

$$\frac{\delta T(\theta, \phi)}{T_0} = \sum_{l \geq 2, m=-l}^{l=\infty, m=l} a_{lm} Y_{lm}(\theta, \phi); \quad (66)$$

where $T_0 = 2.73$ K is the CBR temperature today and the dipole term is subtracted out because it cannot be separated from that arising due to our motion with respect to the cosmic rest frame. The predicted variance due to scalar perturbations is given by

$$\langle |a_{lm}|^2 \rangle = \frac{H_0^4}{2\pi} \int_0^\infty k^{-2} P_S(k) |j_l(kr_0)|^2 dk; \quad (67)$$

$$\simeq \frac{A 2^{n-1} H_0^4 r_0^{1-n}}{16} \frac{\Gamma(l + \frac{1}{2}n - \frac{1}{2}) \Gamma(3-n)}{\Gamma(l - \frac{1}{2}n + \frac{5}{2}) [\Gamma(2 - \frac{1}{2}n)]^2}; \quad (68)$$

where $r_0 \approx 2H_0^{-1}$ is the comoving distance to the last scattering surface, and this expression is for the Sachs-Wolfe contribution from scalar perturbations only. For n not too different from one the expectation for the square of the quadrupole anisotropy is

$$\left(\frac{\Delta T}{T_0} \right)_{Q-S}^2 \equiv \frac{5|a_{2m}|^2}{4\pi} \approx \frac{32\pi}{45} \frac{V_{50}}{m_{\text{Pl}}^4 x_{50}^2} (k_{50} r_0)^{1-n}. \quad (69)$$

(By choosing $k_{50} = r_0^{-1} = \frac{1}{2}H_0$, the last factor becomes unity.)

The ensemble expectation for the multipole amplitudes is often referred to as the angular power spectrum because they encode the full information about predicted CBR anisotropy. For example, the *rms* temperature fluctuation on a given angular scale is related to the multipole amplitudes

$$\left(\frac{\Delta T}{T} \right)_\theta^2 \sim l^2 \langle |a_{lm}|^2 \rangle \quad \text{for } l \simeq 200^\circ/\theta. \quad (70)$$

The procedure for specifying the tensor modes is similar, cf. Refs. [71, 72]. For the modes that enter the horizon after the Universe becomes matter dominated, $k \lesssim 0.1h^2 \text{ Mpc}$, which are the only modes that contribute significantly to CBR anisotropy on angular scales greater than a degree,

$$h_{\mathbf{k}}^i(\tau) = a^i(\mathbf{k}) \left(\frac{3j_1(k\tau)}{k\tau} \right); \quad (71)$$

where $\tau = r_0(t/t_0)^{1/3}$ is conformal time. [For the modes that enter the horizon during the radiation-dominated era, $k \gtrsim 0.1h^2 \text{ Mpc}^{-1}$, the factor $3j_1(k\tau)/k\tau$ is replaced by $j_0(k\tau)$ for the remainder of the radiation era. In either case, the factor involving the

spherical Bessel function quantifies the fact that tensor perturbations remain constant while outside the horizon, and after horizon crossing decrease as R^{-1} .]

The tensor perturbations too are characterized by a gaussian, random variable, here written as $a^i(\mathbf{k})$; the statistical expectation

$$\langle h_{\mathbf{k}}^i h_{\mathbf{q}}^j \rangle = P_T(k) (2\pi)^6 \delta^{(3)}(\mathbf{k} - \mathbf{q}) \delta_{ij}; \quad (72)$$

where the power spectrum

$$P_T(k) = A_T k^{n_T-3} \left[\frac{3j_1(k\tau)}{k\tau} \right]^2; \quad (73)$$

$$A_T = \frac{8}{3\pi} \frac{V_{50}}{m_{\text{Pl}}^4} \frac{(1 + \frac{5}{6}n_T) [\Gamma(\frac{3}{2} - \frac{1}{2}n_T)]^2}{2^{n_T} [\Gamma(\frac{3}{2})]^2} k_{50}^{-n_T}; \quad (74)$$

where the $\mathcal{O}(\alpha_i)$ correction to A_T has been included. Note that $n_T = -2\alpha_T$ is zero for scale-invariant perturbations.

Finally, the contribution of tensor perturbations to the multipole amplitudes, which arise solely due to the Sachs-Wolfe effect [31, 71, 72], is given by

$$\langle |a_{lm}|^2 \rangle \simeq 36\pi^2 \frac{\Gamma(l+3)}{\Gamma(l-1)} \int_0^\infty k^{n_T+1} A_T |F_l(k)|^2 dk; \quad (75)$$

where

$$F_l(k) = - \int_{r_D}^{r_0} dr \frac{j_2(kr)}{kr} \left[\frac{j_l(kr_0 - kr)}{(kr_0 - kr)^2} \right]; \quad (76)$$

and $r_D = r_0/(1+z_D)^{1/2} \approx r_0/35$ is the comoving distance to the horizon at decoupling (= conformal time at decoupling). Equation (75) is approximate in that very short wavelength modes, $kr_0 \gg 100$, that crossed inside the horizon before matter-radiation equality have not been properly taken into account; to take them into account, the integrand must be multiplied by a transfer function,

$$T(k) \simeq 1.0 + 1.44(k/k_{\text{EQ}}) + 2.54(k/k_{\text{EQ}})^2; \quad (77)$$

where $k_{\text{EQ}} \equiv H_0/(2\sqrt{2}-2)R_{\text{EQ}}^{1/2}$ is the scale that entered the horizon at matter radiation equality [68]. In addition, for $l \gtrsim 1000$, the finite thickness of the last-scattering surface must be taken into account.

The tensor contribution to the quadrupole CBR temperature anisotropy for n_T not too different from zero is

$$\left(\frac{\Delta T}{T_0} \right)_{Q-T}^2 \equiv \frac{5|a_{2m}|^2}{4\pi} \simeq 0.61 \frac{V_{50}}{m_{\text{Pl}}^4} (k_{50}r_0)^{-n_T}; \quad (78)$$

where the integrals in the previous expressions have been evaluated numerically.

Both the scalar and tensor contributions to a given multipole are dominated by wavenumbers $kr_0 \sim l$. For scale-invariant perturbations and small l , both the scalar

and tensor contributions to $(l + \frac{1}{2})^2 \langle |a_{lm}|^2 \rangle$ are approximately constant. The contribution of scalar perturbations to $(l + \frac{1}{2})^2 \langle |a_{lm}|^2 \rangle$ begins to decrease for $l \sim 150$ because the scalar contribution to these multipoles is dominated by modes that entered the horizon before matter domination (and hence are suppressed by the transfer function). The contribution of tensor modes to $(l + \frac{1}{2})^2 \langle |a_{lm}|^2 \rangle$ begins to decrease for $l \sim 30$ because the tensor contribution to these multipoles is dominated by modes that entered the horizon before decoupling (and hence decayed as R^{-1} until decoupling). Figure 10 shows the contribution of scalar and tensor perturbations to the CBR anisotropy multipole amplitudes (and includes both the tensor and scalar transfer functions); the expected variance in the CBR multipoles is given by the sum of the scalar and tensor contributions.

3.2 Worked examples

In this Section I apply the formalism developed in the two previous sections to four specific models. So that I can, where appropriate, solve numerically for model parameters, I will: (1) Assume that the astrophysically interesting scales crossed outside the horizon 50 e-folds before the end of inflation; and (2) Use the COBE DMR quadrupole measurement, $\langle (\Delta T)_Q^2 \rangle^{1/2} \approx 20 \pm 2 \mu\text{K}$ [11, 74], to normalize the scalar perturbations; using Eq. (56) this implies

$$V_{50} \approx 2.3 \times 10^{-11} m_{\text{Pl}}^4 x_{50}^2. \quad (79)$$

Of course it is entirely possible that a significant portion of the quadrupole anisotropy is due to tensor-mode perturbations, in which case this normalization must be reduced by a factor of $(1 + T/S)^{-1}$. And, it is straightforward to change “50” to the number appropriate to a specific model, or to normalize the perturbations another way.

Before going on let us use the COBE DMR quadrupole anisotropy to bound the tensor contribution to the quadrupole anisotropy and thereby the energy density that drives inflation:

$$V_{50} \lesssim 7 \times 10^{-11} m_{\text{Pl}}^4. \quad (80)$$

Thus, the upper limit to the tensor contribution to the CBR quadrupole implies that the vacuum energy that drives inflation must be much less than the Planck energy density, indicating that the final 50 or so e-foldings of inflation, which is the relevant part of inflation for us, is not a quantum-gravitational phenomenon. Of course, inflation could last far longer than 50 e-foldings and during the earliest part of inflation the energy density could be Planckian (this is the point of view advocated by Linde in his chaotic inflation model [46]).

3.2.1 Exponential potentials

There are a class of models that can be described in terms of an exponential potential,

$$V(\phi) = V_0 \exp(-\beta\phi/m_{\text{Pl}}). \quad (81)$$

Figure 8: Scalar and tensor contributions to the CBR multipole moments: $l(l+1)\langle|a_{lm}|^2\rangle/6\langle|a_{2m}|^2\rangle$ for the scalar and $l(l+\frac{1}{2})\langle|a_{lm}|^2\rangle/5\langle|a_{2m}|^2\rangle$ for the tensor with $n-1=n_T=0$, $z_{\text{DEC}}=1100$, and $h=0.5$ (from [73]). (The tensor angular power spectrum falls off for $l\sim 30$.) Scale invariance manifests itself in the constancy of the angular power spectra for $l\lesssim 100$. Note, only the Sachs-Wolfe contribution is shown; for scalar perturbations other effects become dominant for $l\gtrsim 100$ and the spectrum rises to a “Doppler peak” at around $l\sim 200$, cf. Fig 3.

This type of potential was first invoked in the context of power-law inflation [75], and has recently received renewed interest in the context of extended inflation [76]. In the simplest model of extended, or first-order, inflation, that based upon the Brans-Dicke-Jordan theory of gravity [76], β is related to the Brans-Dicke parameter: $\beta^2 = 64\pi/(2\omega + 3)$.

For such a potential the slow-roll conditions are satisfied provided that $\beta^2 \lesssim 24\pi$; thus inflation does not end until the potential changes shape, or in the case of extended inflation, until the phase transition takes place. In either case we can relate ϕ_{50} to ϕ_{end} ,

$$N(\phi_{50}) = 50 = \frac{8\pi}{m_{\text{Pl}}^2} \int_{\phi_{50}}^{\phi_{\text{end}}} \frac{V d\phi}{-V'}; \quad \Rightarrow \quad \phi_{50} = \phi_{\text{end}} - 50\beta/8\pi. \quad (82)$$

Since ϕ_{end} is in effect arbitrary, the overall normalization of the potential is irrelevant. The two other parameters, x_{50} and x'_{50} , are easy to compute:

$$x_{50} = -\beta; \quad x'_{50} = 0. \quad (83)$$

Using the COBE DMR normalization, we can relate V_{50} and β :

$$V_{50} = 2.3 \times 10^{-11} m_{\text{Pl}}^4 \beta^2. \quad (84)$$

Further, we can compute q , α_S , α_T , and T/S :

$$q = 16\pi/\beta^2; \quad T/S = 0.28\beta^2; \quad \alpha_T = \alpha_S = 1/(q - 1) \simeq \beta^2/16\pi. \quad (85)$$

Note, for the exponential potential, q , $\alpha_T = \alpha_S$ are independent of epoch. In the case of extended inflation, $\alpha_S = \alpha_T = 4/(2\omega + 3)$; since ω must be less than about 20 [78], this implies significant tilt: $\alpha_S = \alpha_T \gtrsim 0.1$.

3.2.2 Chaotic inflation

The simplest chaotic inflation models are based upon potentials of the form:

$$V(\phi) = a\phi^b; \quad (86)$$

$b = 4$ corresponds to Linde's original model of chaotic inflation and a is dimensionless [46], and $b = 2$ is a model based upon a massive scalar field and $m^2 = 2a$ [79]. In these models ϕ is initially displaced from $\phi = 0$, and inflation occurs as ϕ slowly rolls to the origin. The value of ϕ_{end} is easily found: $\phi_{\text{end}}^2 = b(b - 1)m_{\text{Pl}}^2/24\pi$, and

$$N(\phi_{50}) = 50 = \frac{8\pi}{m_{\text{Pl}}^2} \int_{\phi_{\text{end}}}^{\phi_{50}} \frac{V d\phi}{V'}; \quad (87)$$

$$\Rightarrow \quad \phi_{50}^2/m_{\text{Pl}}^2 = 50b/4\pi + b^2/48\pi \simeq 50b/4\pi; \quad (88)$$

the value of ϕ_{50} is a few times the Planck mass.

For purposes of illustration consider $b = 4$; $\phi_{\text{end}} = m_{\text{Pl}}/\sqrt{2\pi} \simeq 0.4m_{\text{Pl}}$, $\phi_{50} \simeq 4m_{\text{Pl}}$, $\phi_{46} \simeq 3.84m_{\text{Pl}}$, and $\phi_{54} \simeq 4.16m_{\text{Pl}}$. In order to have sufficient inflation the initial value

of ϕ must exceed about $4.2m_{\text{Pl}}$; inflation ends when $\phi \approx 0.4m_{\text{Pl}}$; and the scales of astrophysical interest cross outside the horizon over an interval $\Delta\phi \simeq 0.3m_{\text{Pl}}$.

The values of the potential, its steepness, and the change in steepness are easily found,

$$V_{50} = a m_{\text{Pl}}^b \left(\frac{50b}{4\pi} \right)^{b/2}; \quad x_{50} = \sqrt{\frac{4\pi b}{50}}; \quad m_{\text{Pl}} x'_{50} = \frac{-4\pi}{50}; \quad (89)$$

$$q_{50} = 200/b; \quad T/S = 0.07b; \quad \alpha_T \simeq b/200; \quad \alpha_S = \alpha_T + 0.01. \quad (90)$$

Unless b is very large, scalar perturbations dominate tensor perturbations [80], α_T , α_S are very small, and q is very large. Further, when α_T , α_S become significant, they are equal. Using the COBE DMR normalization we find:

$$a = 2.3 \times 10^{-11} b^{1-b/2} (4\pi/50)^{b/2+1} m_{\text{Pl}}^{4-b}. \quad (91)$$

For the two special cases of interest: $b = 4$, $a = 9 \times 10^{-14}$; and $b = 2$, $m^2 \equiv 2a = 3 \times 10^{-12} m_{\text{Pl}}^2$.

3.2.3 New inflation

These models entail a very flat potential where the scalar field rolls from $\phi \approx 0$ to the minimum of the potential at $\phi = \sigma$. The original models of slow-rollover inflation [81] were based upon potentials of the Coleman-Weinberg form

$$V(\phi) = B\sigma^4/2 + B\phi^4 \left[\ln(\phi^2/\sigma^2) - \frac{1}{2} \right]; \quad (92)$$

where B is a very small dimensionless coupling constant. Other very flat potentials also work (e.g., $V = V_0 - \alpha\phi^4 + \beta\phi^6$ [47]). As before we first solve for ϕ_{50} :

$$N(\phi_{50}) = 50 = \frac{8\pi}{m_{\text{Pl}}^2} \int_{\phi_{\text{end}}}^{\phi_{50}} \frac{V d\phi}{V'}; \quad \Rightarrow \quad \phi_{50}^2 = \frac{\pi\sigma^4}{100 |\ln(\phi_{50}^2/\sigma^2)| m_{\text{Pl}}^2}; \quad (93)$$

where the precise value of ϕ_{end} is not relevant, only the fact that it is much larger than ϕ_{50} . Provided that $\sigma \lesssim m_{\text{Pl}}$, both ϕ_{50} and ϕ_{end} are much less than σ ; we then find

$$V_{50} \simeq B\sigma^4/2; \quad x_{50} \simeq -\frac{(\pi/25)^{3/2}}{\sqrt{|\ln(\phi_{50}^2/\sigma^2)|}} \left(\frac{\sigma}{m_{\text{Pl}}} \right)^2 \ll 1; \quad (94)$$

$$m_{\text{Pl}} x'_{50} \simeq -24\pi/100; \quad q_{50} \simeq \frac{2.5 \times 10^5 |\ln(\phi_{50}^2/\sigma^2)|}{\pi^2} \left(\frac{m_{\text{Pl}}}{\sigma} \right)^4 \gg 1; \quad (95)$$

$$\alpha_T \simeq \frac{1}{q_{50}} \ll 1; \quad \alpha_S = \alpha_T + 0.03; \quad \frac{T}{S} \simeq \frac{6 \times 10^{-4}}{|\ln(\phi_{50}^2/\sigma^2)|} \left(\frac{\sigma}{m_{\text{Pl}}} \right)^4. \quad (96)$$

Provided that $\sigma \lesssim m_{\text{Pl}}$, x_{50} is very small; this means that q is very large, gravity-waves and density perturbations are very nearly scale invariant, and T/S is small. Finally, using the COBE DMR normalization, we can determine the dimensionless coupling constant B :

$$B \simeq 9 \times 10^{-14} / |\ln(\phi_{50}^2/\sigma^2)| \approx 4 \times 10^{-15}. \quad (97)$$

3.2.4 Natural inflation

This model is based upon a potential of the form [55]

$$V(\phi) = \Lambda^4 [1 + \cos(\phi/f)]. \quad (98)$$

The flatness of the potential (and requisite small couplings) arise because the ϕ particle is a pseudo-Nambu-Goldstone boson (f is the scale of spontaneous symmetry breaking and Λ is the scale of explicit symmetry breaking; in the limit that $\Lambda \rightarrow 0$ the ϕ particle is a massless Nambu-Goldstone boson). It is a simple matter to show that ϕ_{end} is of the order of πf .

This potential is difficult to analyze in general; however, there are two limiting regimes: (i) $f \gg m_{\text{Pl}}$; and (ii) $f \lesssim m_{\text{Pl}}$ [47]. In the first regime, the 50 or so relevant e-folds take place close to the minimum of the potential, $\sigma = \pi f$, and inflation can be analyzed by expanding the potential about $\phi = \sigma$,

$$V(\psi) \simeq m^2 \psi^2 / 2; \quad (99)$$

$$m^2 = \Lambda^4 / f^2; \quad \psi = \phi - \sigma. \quad (100)$$

In this regime natural inflation is equivalent to chaotic inflation with $m^2 = \Lambda^4 / f^2 \simeq 3 \times 10^{-12} m_{\text{Pl}}^2$.

In the second regime, $f \lesssim m_{\text{Pl}}$, inflation takes place when $\phi \lesssim \pi f$, so that we can make the following approximations: $V \simeq 2\Lambda^4$ and $V' = -\Lambda^4 \phi / f^2$. Taking $\phi_{\text{end}} \sim \pi f$, we can solve for $N(\phi)$:

$$N(\phi) = \frac{8\pi}{m_{\text{Pl}}^2} \int_{\phi}^{\pi f} \frac{V d\phi}{-V'} \simeq \frac{16\pi m_{\text{Pl}}^2}{f^2} \ln(\pi f / \phi); \quad (101)$$

from which it is clear that achieving 50 e-folds of inflation places a lower bound to f , very roughly $f \gtrsim m_{\text{Pl}}/3$ [47, 55].

Now we can solve for ϕ_{50} , V_{50} , x_{50} , and x'_{50} :

$$\phi_{50} / \pi f \simeq \exp(-50 m_{\text{Pl}}^2 / 16\pi f^2) \lesssim \mathcal{O}(0.1); \quad V_{50} \simeq 2\Lambda^4; \quad (102)$$

$$x_{50} \simeq \frac{1}{2} \frac{m_{\text{Pl}}}{f} \frac{\phi_{50}}{f} \lesssim \mathcal{O}(0.1); \quad x'_{50} \simeq -\frac{1}{2} \left(\frac{m_{\text{Pl}}}{f} \right)^2. \quad (103)$$

Using the COBE DMR normalization, we can relate Λ to f/m_{Pl} :

$$\Lambda / m_{\text{Pl}} = 7 \times 10^{-4} \sqrt{\frac{m_{\text{Pl}}}{f}} \exp(-25 m_{\text{Pl}}^2 / 16\pi f^2). \quad (104)$$

Further, we can solve for T/S , α_T , and α_S :

$$\frac{T}{S} \simeq 0.07 \left(\frac{m_{\text{Pl}}}{f} \right)^2 \left(\frac{\phi_{50}}{f} \right)^2 \lesssim \mathcal{O}(0.1); \quad (105)$$

$$\alpha_T = \frac{1}{16\pi} \frac{q_{50}}{q_{50} - 1} \left(\frac{1}{4} \frac{m_{\text{Pl}}^2}{f^2} \frac{\phi_{50}^2}{f^2} \right) \approx \frac{1}{64\pi} \left(\frac{m_{\text{Pl}}}{f} \right)^2 \left(\frac{\phi_{50}}{f} \right)^2 \ll 0.1; \quad (106)$$

$$\alpha_S = \frac{1}{16\pi} \frac{q_{50}}{q_{50} - 1} \left(\frac{1}{4} \frac{m_{\text{Pl}}^2}{f^2} \frac{\phi_{50}^2}{f^2} + \frac{m_{\text{Pl}}^2}{f^2} \right) \approx \frac{1}{16\pi} \left(\frac{m_{\text{Pl}}}{f} \right)^2; \quad (107)$$

$$q_{50} = 64\pi \left(\frac{f}{m_{\text{Pl}}} \right)^2 \left(\frac{f}{\phi_{50}} \right)^2 \gg 1. \quad (108)$$

Regime (ii) provides the exception to the rule that $\alpha_S \approx \alpha_T$ and large α_S implies large T/S . For example, taking $f = m_{\text{Pl}}/2$, we find:

$$\phi_{50}/f \sim 0.06; \quad x_{50} \sim 0.06; \quad x'_{50} = -2; \quad q_{50} \sim 10^4; \quad (109)$$

$$\alpha_T \sim 10^{-4}; \quad \alpha_S \sim 0.08; \quad T/S \sim 10^{-3}. \quad (110)$$

The gravitational-wave perturbations are very nearly scale invariant, while the density perturbations deviate significantly from scale invariance. I note that regime (ii), i.e., $f \lesssim m_{\text{Pl}}$, occupies only a tiny fraction of parameter space because f must be greater than about $m_{\text{Pl}}/3$ to achieve sufficient inflation; further, regime (ii) is “fine tuned” and “unnatural” in the sense that the required value of Λ is exponentially sensitive to the value of f/m_{Pl} .

Finally, I note that the results for regime (ii) apply to any inflationary model whose Taylor expansion in the inflationary region is similar; e.g., $V(\phi) = -m^2\phi^2 + \lambda\phi^4$, which was originally analyzed in Ref. [47].

3.2.5 Lessons

To summarize the general features of our results. In all examples the deviations from scale invariance enhance perturbations on large scales. The only potentials that have significant deviations from scale invariance are either very steep or have rapidly changing steepness. In the former case, both the scalar and tensor perturbations are tilted by a similar amount; in the latter case, only the scalar perturbations are tilted.

For “steep” potentials, the expansion rate is “slow,” i.e., q_{50} close to unity, the gravity-wave contribution to the CBR quadrupole anisotropy becomes comparable to, or greater than, that of density perturbations, and both scalar and tensor perturbations are tilted significantly. For flat potentials, i.e., small x_{50} , the expansion rate is “fast,” i.e., $q_{50} \gg 1$, the gravity-wave contribution to the CBR quadrupole is much smaller than that of density perturbations, and unless the steepness of the potential changes significantly, large x'_{50} , both spectra very nearly scale invariant; if the steepness of the potential changes rapidly, the spectrum of scalar perturbations can be tilted significantly. The models that permit significant deviations from scale invariance involve exponential or low-order polynomial potentials; the former by virtue of their steepness, the latter by virtue of the rapid variation of their steepness. Exponential potentials are of interest because they arise in extended inflation models; potentials with rapidly steepness include $V(\phi) = -m^2\phi^2 + \lambda\phi^4$ or $\Lambda^4[1 + \cos(\phi/f)]$.

Finally, to illustrate how observational data could be used to determine the properties of the inflationary potential and test the consistency of the inflationary hypothesis, suppose observations determined the following:

$$(\Delta T)_Q \simeq 16\mu\text{K}; \quad T/S = 0.24; \quad n = 0.9; \quad (111)$$

that is, the COBE DMR quadrupole anisotropy, a four to one ratio of scalar to tensor contribution to the CBR quadrupole, and spectral index of 0.9 for the scalar perturbations. From T/S , we determine the steepness of the potential: $x_{50} \simeq 0.94$. From the steepness and the quadrupole anisotropy the value of the potential: $V_{50}^{1/4} \simeq 2.4 \times 10^{16} \text{ GeV}$. From the spectral index the change in steepness: $x'_{50} \simeq -0.81/m_{\text{Pl}}$. These data can also be expressed in terms of the value of the potential and its first two derivatives:

$$V_{50} = 1.4 \times 10^{-11} m_{\text{Pl}}^4; \quad V'_{50} = 1.5 \times 10^{-11} m_{\text{Pl}}^3; \quad V''_{50} = 1.0 \times 10^{-12} m_{\text{Pl}}^2. \quad (112)$$

Further, they lead to the prediction: $n_T = -0.035$, which, when “measured,” can be used as a consistency check for inflation.

4 STRUCTURE FORMATION: CRUCIAL TEST OF INFLATION

The key to testing inflation is to focus on its robust predictions and their implications. Earlier I discussed the prediction of a flat Universe and its bold implication that most of the matter in Universe exists in the form of particle dark matter. Much effort is being directed at determining the mean density of the Universe and detecting particle dark matter.

The scale-invariant scalar metric perturbations lead to CBR anisotropy on angular scales from less than 1° to 90° and seed the formation of structure in the Universe. Together with the nucleosynthesis determination of Ω_B and the inflationary prediction of a flat Universe, scale-invariant density perturbations lead to a very specific scenario for structure formation; it is known as cold dark matter because the bulk of the particle dark matter is comprised of slowly moving particles (e.g., axions or neutralinos) [82].⁸ A large and rapidly growing number of observations are being brought

⁸The simpler possibility, that the particle dark matter exists in the form of 30 eV or so neutrinos which is known as hot dark matter, was falsified almost a decade ago. Because neutrinos move rapidly, they can diffuse from high density to low density regions damping perturbations on small scales. In hot dark matter large, supercluster-size objects must form before galaxies, and thus hot dark matter cannot account for the abundance of galaxies, damped Lyman- α clouds, etc. that is observed at high redshift.

to bear in the testing of cold dark matter, making it the centerpiece of efforts to test inflation.

Finally, there are the scale-invariant tensor perturbations. They lead to CBR anisotropy on angular scales from a few degrees to 90° and a spectrum of gravitational waves. The CBR anisotropy arising from the tensor perturbations can in principle be separated from that arising from scalar perturbations. However, because the sky is finite, sampling variance sets a fundamental limit: the tensor contribution to CBR anisotropy can only be separated from that of the scalar if T/S is greater than about 0.14 [83]. It is also possible that the stochastic background of gravitational waves itself can be directly detected, though it appears that the LIGO facilities being built will lack the sensitivity and even space-based interferometry (e.g., LISA) is not a sure bet [84].

Before going on to discuss how cold dark matter models are testing inflation I want to emphasize the importance of the tensor perturbations. The attractiveness of a flat Universe with scale-invariant density perturbations was appreciated long before inflation. Verifying these two predictions of inflation, while important, will not provide a “smoking gun.” The tensor perturbations are a unique feature of inflation. Further, they are crucial to obtaining information about the scalar potential responsible for inflation.

4.1 Vanilla Cold Dark Matter: almost, but not quite?

Cold dark matter has often been characterized as a “no parameter model” for structure formation; that is only true in the broad brush: cold dark matter is characterized by scale-invariant density perturbations and a matter content that is almost entirely slowly moving particles. To make predictions of the precision needed to match current observations, a more specific characterization is essential – precise power-law index of the spectrum of density perturbations, amplitude of tensor perturbations, Hubble constant, baryon density, radiation content of the Universe, possible cosmological constant, and so on.

Historically, the “standard” version of cold dark matter, vanilla cold dark matter if you will, is : (1) $\Omega_B \simeq 0.05$ and $\Omega_{\text{CDM}} \sim 0.95$; (2) Hubble constant of $50 \text{ km s}^{-1} \text{ Mpc}^{-1}$; (3) Precisely scale-invariant density perturbations ($n = 1$); and (4) No contribution of tensor perturbations to CBR anisotropy. Standard cold dark matter has no other significance than as a default starting point. Because it became an “industry standard” vanilla cold dark matter provides an interesting point of comparison – but that is all!

In cold dark matter models structure forms hierarchically, with small objects forming first and merging to form larger objects. Galaxies form at redshifts of order a few, and rarer objects like QSOs form from higher than average density peaks earlier. In general, cold dark matter predicts a Universe that is still evolving at recent epochs. N -body simulations are crucial to bridging the gap between theory and observation, and several groups have carried out large numerical studies of vanilla cold dark matter

[85].

There are a diversity of observations that test cold dark matter; they include CBR anisotropy and spectral distortions, redshift surveys, pairwise velocities of galaxies, peculiar velocities, redshift space distortions, x-ray background, QSO absorption line systems, cluster studies of all kinds, studies of evolution (clusters, galaxies, and so on), measurements of the Hubble constant, and on and on. I will focus on how these measurements probe the power spectrum of density perturbations, emphasizing the role of CBR-anisotropy measurements and redshift surveys.

Density perturbations on a (comoving) length scale λ give rise to CBR anisotropy on an angular scale $\theta \sim \lambda/H_0^{-1} \sim 1^\circ(\lambda/100h^{-1}\text{Mpc})$.⁹ CBR anisotropy has now been detected by more than ten experiments on angular scales from about 0.5° to 90° , thereby probing length scales from $30h^{-1}\text{Mpc}$ to 10^4h^{-1}Mpc . The very accurate measurements made by the COBE DMR can be used to normalize the cold dark matter spectrum (the normalization scale corresponds to about 20°). When this is done, the other ten or so measurements are in agreement with the predictions of cold dark matter (see Fig. 1).

The COBE-normalized cold dark matter spectrum can be extrapolated to the much smaller scales probed by redshift surveys, from about $1h^{-1}\text{Mpc}$ to $100h^{-1}\text{Mpc}$. When this is done, there is general agreement. However, on closer inspection the COBE-normalized spectrum seems to predict excess power on these scales (about a factor of four in the power spectrum; see Fig. 7). This conclusion is supported by other observations, e.g., the abundance of rich clusters and the pairwise velocities of galaxies. It suggests that cold dark matter has much of the truth, but perhaps not all of it [86], and has led to the suggestion that something needs to be added to the simplest cold dark matter theory.

There is another important challenge facing cold dark matter. X-ray observations of rich clusters are able to determine the ratio of hot gas (baryons) to total cluster mass (baryons + CDM) (by a wide margin, most of the baryons “seen” in clusters are in the hot gas). To be sure there are assumptions and uncertainties; the data at the moment indicate that this ratio is $(0.04 - 0.08)h^{-3/2}$ [22]. If clusters provide a fair sample of the universal mix of matter, then this ratio should equal $\Omega_B/(\Omega_B + \Omega_{\text{CDM}}) \simeq (0.009 - 0.022)h^{-2}/(\Omega_B + \Omega_{\text{CDM}})$. Since clusters are large objects they should provide a pretty fair sample. Taking the numbers at face value, cold dark matter is consistent with the cluster gas fraction provided either: $\Omega_B + \Omega_{\text{CDM}} = 1$ and $h \sim 0.3$ or $\Omega_B + \Omega_{\text{CDM}} \sim 0.3$ and $h \sim 0.7$. The cluster baryon problem has yet to be settled, and is clearly an important test of cold dark matter.

Finally, before going on to discuss the variants of cold dark matter now under consideration, let me add a note of caution. The comparison of predictions for structure formation with present-day observations of the distribution of galaxies is fraught with difficulties. Theory most accurately predicts “where the mass is” (in a statisti-

⁹For reference, perturbations on a length scale of about 1 Mpc give rise to galaxies, on about 10 Mpc to clusters, on about 30 Mpc to large voids, and on about 100 Mpc to the great walls.

cal sense) and the observations determine where the light is. Redshift surveys probe present-day inhomogeneity on scales from around one Mpc to a few hundred Mpc, scales where the Universe is nonlinear ($\delta n_{\text{GAL}}/n_{\text{GAL}} \gtrsim 1$ on scales $\lesssim 8h^{-1}$ Mpc) and where astrophysical processes undoubtedly play an important role (e.g., star formation determines where and when “mass lights up,” the explosive release of energy in supernovae can move matter around and influence subsequent star formation, and so on). The distance to a galaxy is determined through Hubble’s law ($d = H_0^{-1}z$) by measuring a redshift; peculiar velocities induced by the lumpy distribution of matter are significant and prevent a direct determination of the actual distance. There are the intrinsic limitations of the surveys themselves: they are flux not volume limited (brighter objects are seen to greater distances and vice versa) and relatively small (e.g., the CfA slices of the Universe survey contains only about 10^4 galaxies and extends to a redshift of about $z \sim 0.03$). Last but not least are the numerical simulations which link theory and observation; they are limited in dynamical range (about a factor of 100 in length scale) and in microphysics (in the largest simulations only gravity, and in others only a gross approximation to the effects of hydrodynamics/thermodynamics). Perhaps it would be prudent to withhold judgment on vanilla cold dark matter for the moment and resist the urge to modify it—but that wouldn’t be as much fun!

4.2 The many flavors of cold dark matter

The spectrum of density perturbations today depends not only upon the primeval spectrum (and the normalization on large scales provided by COBE), but also upon the energy content of the Universe. While the fluctuations in the gravitational potential were initially (approximately) scale invariant, the Universe evolved from an early radiation-dominated phase to a matter-dominated phase which imposes a characteristic scale on the spectrum of density perturbations seen today; that scale is determined by the energy content of the Universe, $k_{\text{EQ}} \sim 10^{-1}h \text{ Mpc}^{-1}$ ($\Omega_{\text{matter}}h/\sqrt{g_*}$) (g_* counts the relativistic degrees of freedom, $\Omega_{\text{matter}} = \Omega_B + \Omega_{\text{CDM}}$). In addition, if some of the nonbaryonic dark matter is neutrinos, they reduce power on small scales somewhat through freestreaming (see Fig. 7). With this in mind, let me discuss the variants of cold dark matter that have been proposed to improve its agreement with observations.

1. **Low Hubble Constant + cold dark matter (LHC CDM) [87].** Remarkably, simply lowering the Hubble constant to around $30 \text{ km s}^{-1} \text{ Mpc}^{-1}$ solves all the problems of cold dark matter. Recall, the critical density $\rho_{\text{crit}} \propto H_0^2$; lowering H_0 lowers the matter density and has precisely the desired effect. It has two other added benefits: the expansion age of the Universe is comfortably consistent with the ages of the oldest stars and the baryon fraction is raised to a value that is consistent with that measured in x-ray clusters. Needless to say, such a small value for the Hubble constant flies in the face of current observations [5, 6]; further, it illustrates that the problems of cold dark matter get even worse for the larger values of H_0 that are favored by recent observations.

2. **Hot + cold dark matter (ν CDM) [88].** Adding a small amount of hot dark matter can suppress density perturbations on small scales; adding too much leads back to the longstanding problems of hot dark matter. Retaining enough power on very small scales to produce damped Lyman- α systems at high redshift limits Ω_ν to less than about 20%, corresponding to about “5 eV worth of neutrinos” (i.e., one species of mass 5 eV, or two species of mass 2.5 eV, and so on). This admixture of hot dark matter rejuvenates cold dark matter provided the Hubble constant is not too large, $H_0 \lesssim 55 \text{ km s}^{-1} \text{ Mpc}^{-1}$; in fact, a Hubble constant of closer to $45 \text{ km s}^{-1} \text{ Mpc}^{-1}$ is preferred.
3. **Cosmological constant + cold dark matter (Λ CDM) [89].** (A cosmological constant corresponds to a uniform energy density, or vacuum energy.) Shifting 50% to 70% of the critical density to a cosmological constant lowers the matter density and has the same beneficial effect as a low Hubble constant. In fact, a Hubble constant as large as $80 \text{ km s}^{-1} \text{ Mpc}^{-1}$ can be accommodated. In addition, the cosmological constant allows the age problem to be solved even if the Hubble constant is large, addresses the fact that few measurements of the mean mass density give a value as large as the critical density (most measurements of the mass density are insensitive to a uniform component), and allows the baryon fraction of matter to be larger, which alleviates the cluster baryon problem. Not everything is rosy; cosmologists have invoked a cosmological constant twice before to solve their problems (Einstein to obtain a static universe and Bondi, Gold, and Hoyle to solve the earlier age crisis when H_0 was thought to be $250 \text{ km s}^{-1} \text{ Mpc}^{-1}$). Further, particle physicists can still not explain why the energy of the vacuum is not at least 50 (if not 120) orders of magnitude larger than the present critical density, and expect that when the problem is solved the answer will be zero.
4. **Extra relativistic particles + cold dark matter (τ CDM) [90].** Raising the level of radiation has the same beneficial effect as lowering the matter density. In the standard cosmology the radiation content consists of photons + three (undetected) cosmic seas of neutrinos (corresponding to $g_* \simeq 3.36$). While we have no direct determination of the radiation beyond that in the CBR, there are at least two problems: What are the additional relativistic particles? and Can additional radiation be added without upsetting the successful predictions of primordial nucleosynthesis which depend critically upon the energy density of relativistic particles? The simplest way around these problems is an unstable tau neutrino (mass anywhere between a few keV and a few MeV) whose decays produce the radiation. This fix can tolerate a larger Hubble constant, though at the expense of more radiation.
5. **Tilted cold dark matter (TCDM) [91].** While the spectrum of density perturbations in most models of inflation is very nearly scale invariant, there are models where the deviations are significant ($n \approx 0.8$) which leads to smaller fluctuations on small scales. Further, if gravity waves account for a significant

part of the CBR anisotropy, the level of density perturbations can be lowered even more. A combination of tilt and gravity waves can solve the problem of too much power on small scales, but seems to lead to too little power on intermediate and very small scales.

These possibilities represent different approaches to improving the concordance of CDM. They also represent well motivated modifications to the standard cosmology in their own right. It has always been appreciated that the inflationary spectrum of density perturbations was not exactly scale invariant [47] and that the Hubble constant was unlikely to be exactly $50 \text{ km s}^{-1} \text{ Mpc}$. Neutrinos exist; they are expected to have mass; there is even some experimental data that indicates they do have mass [92]. If the Hubble constant is as large as $70 \text{ km s}^{-1} \text{ Mpc}^{-1}$ to $80 \text{ km s}^{-1} \text{ Mpc}^{-1}$ a cosmological constant seems inescapable based upon the age of the Universe alone. There is no data precludes more radiation than in the standard cosmology. In fact, these modifications to vanilla cold dark matter are so well motivated that one should probably also consider combinations; e.g., lesser tilt and $h = 0.45$ and so on [93].

In evaluating these better fit models, one should keep the words of Francis Crick in mind (loosely paraphrased): A model that fits all the data at a given time is necessarily wrong, because at any given time not all the data are correct(!). Λ CDM provides an interesting/confusing example. When I discussed it in 1990, I called it the best-fit Universe, and quoting Crick, I said that Λ CDM was certain to fall by the wayside [94]. In 1995, it is still the best-fit model [95].

4.3 Reconstruction

If inflation and the cold dark matter theory is shown to be correct, then a window to the very early Universe ($t \sim 10^{-34} \text{ sec}$) will have been opened. While it is certainly premature to jump to this conclusion, I would like to illustrate one example of what one could hope to learn. As mentioned earlier, the spectra and amplitudes of the the tensor and scalar metric perturbations predicted by inflation depend upon the underlying model, to be specific, the shape of the inflationary scalar-field potential. If one can measure the power-law index of the scalar spectrum and the amplitudes of the scalar and tensor spectra, one can recover the value of the potential and its first two derivatives around the point on the potential where inflation took place [96]:

$$V = 1.65 T m_{\text{Pl}}^4, \quad (113)$$

$$V' = \pm \sqrt{\frac{8\pi r}{7}} V/m_{\text{Pl}}, \quad (114)$$

$$V'' = 4\pi \left[(n-1) + \frac{3}{7}r \right] V/m_{\text{Pl}}^2, \quad (115)$$

where $r \equiv T/S$, a prime indicates derivative with respect to ϕ , $m_{\text{Pl}} = 1.22 \times 10^{19} \text{ GeV}$ is the Planck energy, and the sign of V' is indeterminate. In addition, if the tensor

spectral index can be measured a consistency relation, $n_T = -r/7$, can be used to further test inflation. Reconstruction of the inflationary scalar potential would shed light both on inflation as well as physics at energies of the order of 10^{15} GeV. (If $\Lambda \neq 0$, these expressions are modified [97].)

5 The Future

The stakes for cosmology are high: if correct, inflation/cold dark matter represents a major extension of the big bang and our understanding of the Universe. Further, it will shed light on the fundamental physics at energies of order 10^{15} GeV.

What are the crucial tests and when will they be carried out? Because of the many measurements/observations that can have significant impact, I believe the answer to when is sooner rather than later. The list of pivotal observations is long: CBR anisotropy, large redshift surveys (e.g., the Sloan Digital Sky Survey will have 10^6 redshifts), direct searches for nonbaryonic in our neighborhood (both for axions and neutralinos) and baryonic dark matter (microlensing), x-ray studies of galaxy clusters, the use of back-lit gas clouds (quasar absorption line systems) to study the Universe at high redshift, evolution (as revealed by deep images of the sky taken by the Hubble Space Telescope and the Keck 10 meter telescope), measurements of both H_0 and q_0 , mapping of the peculiar velocity field at large redshifts through the Sunyaev-Zel'dovich effect, dynamical estimates of the mass density (using weak gravitational lensing, large-scale velocity fields, and so on), age determinations, gravitational lensing, searches for supersymmetric particles (at accelerators) and neutrino oscillations (at accelerators, solar-neutrino detectors, and other large underground detectors), searches for high-energy neutrinos from neutralino annihilations in the sun using large underground detectors, and on and on. Let me end by illustrating the interesting consequences of several possible measurements.

A definitive determination that H_0 is greater than $55 \text{ km s}^{-1} \text{ Mpc}^{-1}$ would falsify all CDM models except that with a cosmological constant and would certainly give particle theorists something to think about. (A definitive determination that H_0 is $75 \text{ km s}^{-1} \text{ Mpc}^{-1}$ or larger would necessitate a cosmological constant based upon the age of the Universe alone, though it should be noted that none of the CDM models consistent with large-scale structure have an age problem.) A flat Universe with a cosmological constant has a very different deceleration parameter than one dominated by matter, $q_0 = -1.5\Omega_\Lambda + 0.5 \sim -(0.4 - 0.7)$ compared to $q_0 = 0.5$, and this could be settled by galaxy-number counts, quasar-lensing statistics, or a Hubble diagram based upon Type Ia supernovae. The predicted CBR anisotropy on the 0.5° scale in τ CDM and LHC CDM is about 50% larger than vanilla CDM and about 50% smaller in TCDM, which should be easily discernible. If neutrino-oscillation experiments were to provide evidence for a neutrino of mass 5 eV (or two of mass 2.5 eV) ν CDM would seem almost inescapable [92].

More CBR measurements are in progress and there should many interesting results

in the next few years. In the wake of the success of COBE there are proposals, both in the US and Europe, for a satellite-borne instrument to map the CBR sky with a factor of thirty or more better resolution. A map of the CBR with 0.3° resolution could separate the gravity-wave contribution to CBR anisotropy and provide evidence for the third robust prediction of inflation, as well as determining other important parameters [98], e.g., the scalar and tensor indices, Ω_Λ , and even Ω_0 (the position of the “Doppler” peak scales as $\sqrt{\Omega_0}$ degrees [99]).

The future in cosmology is very bright: We have a highly successful standard model—the hot big-bang; bold ideas for extending it—inflation and cold dark matter; and a flood of data to test these ideas.

References

- [1] For a textbook treatment of the standard cosmology see e.g., S. Weinberg, *Gravitation and Cosmology* (Wiley, NY, 1972); E.W. Kolb and M.S. Turner, *The Early Universe* (Addison-Wesley, Redwood City, CA, 1990).
- [2] A. Sandage, *Physica Scripta* **T43**, 22 (1992).
- [3] J. Mould et al., *Astrophys. J.* **383**, 467 (1991).
- [4] See e.g., M. Rowan-Robinson, *The Cosmological Distance Ladder* (Freeman, San Francisco, 1985).
- [5] M. Fukugita, C.J. Hogan, and P.J.E. Peebles, *Nature* **366**, 309 (1993); G. Jacoby et al, *Proc. Astron. Soc. Pac.* **104**, 599 (1992); A. Reiss, R.P. Krishner, and W. Press, *Astrophys. J.* **438**, L17 (1995); M. Hamuy et al, *Astron. J.* **109**, 1 (1995).
- [6] W. Freedman et al., *Nature* **371**, 757 (1994).
- [7] J. Mather et al., *Astrophys. J.* **420**, 439 (1993).
- [8] P.J.E. Peebles, D.N. Schramm, E. Turner, and R. Kron, *Nature* **352**, 769 (1991).
- [9] G.F. Smoot et al., *Astrophys. J.* **396**, L1 (1992); A. Kogut et al., *ibid* **419**, 1 (1993).
- [10] G.F. Smoot, in *First Course in Current Topics in Astrophundamental Physics*, eds. N. Sanchez and A. Zichichi (World Scientific, Singapore, 1992), p. 192.
- [11] G.F. Smoot et al., *Astrophys. J.* **396**, L1 (1992); E.L. Wright, *ibid* **396**, L3 (1992).

- [12] M. White, D. Scott, and J. Silk, *Ann. Rev. Astron. Astrophys.* **32**, 319 (1994); *Science* **268**, 829 (1995).
- [13] T.P. Walker et al., *Astrophys. J.* **376**, 51 (1991).
- [14] C. Copi, D.N. Schramm, and M.S. Turner, *Science* **267**, 192 (1995).
- [15] L.M. Krauss and P. Kernan, *Phys. Lett. B* **347**, 347 (1995).
- [16] C. Copi, D.N. Schramm, and M.S. Turner, *Phys. Rev. Lett.* **75**, xxx (1995).
- [17] E.W. Kolb et al., *Phys. Rev. Lett.* **67**, 533 (1991).
- [18] S. Dodelson, G. Gyuk, and M.S. Turner, *Phys. Rev. D* **49**, 5068 (1994).
- [19] See e.g., M. Bolte and C.J. Hogan, *Nature* **376**, 399 (1995); J. Cowan, F. Thieleman, and J. Truran, *Ann. Rev. Astron. Astrophys.* —bf 29, 447 (1991).
- [20] For recent reviews of dark matter see e.g., M.S. Turner, *Physica Scripta* **T36**, 167 (1991); P.J.E. Peebles, *Nature* **321**, 27 (1986); V. Trimble, *Ann. Rev. Astron. Astrophys.* **25**, 425 (1987); J. Kormendy and G. Knapp, *Dark Matter in the Universe* (Reidel, Dordrecht, 1989); K. Ashman, *Proc. Astron. Soc. Pac.* **104**, 1109 (1992); S. Faber and J. Gallagher, *Ann. Rev. Astron. Astrophys.* **17**, 135 (1979).
- [21] See e.g., N. Kaiser, astro-ph/9509019.
- [22] S.D.M. White et al., *Nature* **366**, 429 (1993); U.G. Briel et al., *Astron. Astrophys.* **259**, L31 (1992); D.A. White and A.C. Fabian, *Mon. Not. R. astron. Soc.* **273**, 72 (1995).
- [23] M. Rowan-Robinson et al., *Mon. Not. R. astr. Soc.* **247**, 1 (1990); N. Kaiser et al., *ibid* **252**, 1 (1991); M. Strauss et al., *Astrophys. J.* **385**, 444 (1992).
- [24] A. Dekel, *Ann. Rev. Astron. Astrophys.* **32**, 319 (1994).
- [25] A. Sandage, *Astrophys. J.* **133**, 355 (1961); *Physica Scripta* **T43**, 7 (1992); Refs. [1].
- [26] E. Loh and E. Spillar, *Astrophys. J.* **307**, L1 (1986); M. Fukugita et al., *ibid* **361**, L1 (1990).
- [27] See e.g., E.W. Kolb and M.S. Turner, *Ann. Rev. Nucl. Part. Sci.* **33**, 645 (1983); A. Dolgov, *Phys. Repts.*, in press (1993); A. Cohen, D. Kaplan, and A. Nelson, *Ann. Rev. Nucl. Part. Sci.* **43**, 27 (1992).
- [28] S. Weinberg, *Gravitation and Cosmology* (Wiley, NY, 1972).

- [29] For a more complete pedagogical discussion of structure formation see e.g., Refs. [1]; P.J.E. Peebles, *The Large-scale Structure of the Universe* (Princeton Univ. Press, Princeton, 1980); G. Efstathiou, in *The Physics of the Early Universe*, eds. J.A. Peacock, A.F. Heavens, and A.T. Davies (Adam-Higler, Bristol, 1990).
- [30] For a pedagogical discussion of CBR anisotropy see e.g., G. Efstathiou, in *The Physics of the Early Universe*, eds. J.A. Peacock, A.F. Heavens, and A.T. Davies (Adam-Higler, Bristol, 1990). Also see, J.R. Bond and G. Efstathiou, *Mon. Not. R. astr. Soc.* **226**, 655 (1987); J.R. Bond et al., *Phys. Rev. Lett.* **66**, 2179 (1991).
- [31] R.K. Sachs and A.M. Wolfe, *Astrophys. J.* **147**, 73 (1967).
- [32] W. Hu and N. Sugiyama, *Phys. Rev. D* **51**, 2599 (1995).
- [33] P.J.E. Peebles, *Nature* **327**, 210 (1987); *Astrophys. J.* **315**, L73 (1987); R. Cen, J.P. Ostriker, and P.J.E. Peebles, *ibid* **415**, 423 (1993).
- [34] See e.g., A. Vilenkin, *Phys. Repts.* **121**, 263 (1985); A. Albrecht and A. Stebbins, *Phys., Rev. Lett.* **69**, 2615 (1992); D. Bennett, A. Stebbins, and F. Bouchet, *Astrophys. J.* **399**, L5 (1992).
- [35] See e.g., N. Turok, *Phys. Rev. Lett.* **63**, 2652 (1989); A. Gooding, D. Spergel, and N. Turok, *Astrophys. J.* **372**, L5 (1991).
- [36] C.B. Collins and S.W. Hawking, *Astrophys. J.* **180**, 317 (1973).
- [37] E.W. Kolb and M.S. Turner, *The Early Universe* (Addison-Wesley, Redwood City, CA, 1990).
- [38] Y. Hu, M.S. Turner, and E.J. Weinberg, *Phys. Rev. D* **49**, 3830 (1994).
- [39] A. H. Guth and S.-Y. Pi, *Phys. Rev. Lett.* **49**, 1110 (1982); S. W. Hawking, *Phys. Lett. B* **115**, 295 (1982); A. A. Starobinskii, *ibid* **117**, 175 (1982); J. M. Bardeen, P. J. Steinhardt, and M. S. Turner, *Phys. Rev. D* **28**, 697 (1983).
- [40] V.A. Rubakov, M. Sazhin, and A. Veryaskin, *Phys. Lett. B* **115**, 189 (1982); R. Fabbri and M. Pollock, *ibid* **125**, 445 (1983); A.A. Starobinskii *Sov. Astron. Lett.* **9**, 302 (1983); L. Abbott and M. Wise, *Nucl. Phys. B* **244**, 541 (1984).
- [41] M.S. Turner and L.M. Widrow, *Phys. Rev. Lett.* **57**, 2237 (1986); L. Jensen and J. Stein-Schabes, *Phys. Rev. D* **35**, 1146 (1987); A.A. Starobinskii, *JETP Lett.* **37**, 66 (1983).

- [42] A.D. Linde, *Inflation and Quantum Cosmology* (Academic Press, San Diego, CA, 1990).
- [43] A.H. Guth, *Phys. Rev. D* **23**, 347 (1981).
- [44] A.D. Linde, *Phys. Lett. B* **108**, 389 (1982).
- [45] A. Albrecht and P.J. Steinhardt, *Phys. Rev. Lett.* **48**, 1220 (1982).
- [46] A.D. Linde, *Phys. Lett. B* **129**, 177 (1983).
- [47] P.J. Steinhardt and M.S. Turner, *Phys. Rev. D* **29**, 2162 (1984).
- [48] Q. Shafi and A. Vilenkin, *Phys. Rev. Lett.* **52**, 691 (1984); S.-Y. Pi, *ibid* **52**, 1725 (1984).
- [49] R. Holman, P. Ramond, and G.G. Ross, *Phys. Lett. B* **137**, 343 (1984).
- [50] K. Olive, *Phys. Repts.* **190**, 309 (1990).
- [51] H. Murayama et al., *Phys. Rev. D(RC)* **50**, R2356 (1994).
- [52] M. Cvetič, T. Hubsch, J. Pati, and H. Stremnitzer, *Phys. Rev. D* **40**, 1311 (1990).
- [53] E.J. Copeland et al., *Phys. Rev. D* **49**, 6410 (1994).
- [54] See e.g., M. Gasperini and G. Veneziano, *Phys. Rev. D* **50**, 2519 (1994); R. Brustein and G. Veneziano, *Phys. Lett. B* **329**, 429 (1994); T. Banks et al., hep-th/9503114.
- [55] K. Freese, J.A. Frieman, and A. Olinto, *Phys. Rev. Lett.* **65**, 3233 (1990).
- [56] L. Knox and M.S. Turner, *Phys. Rev. Lett.* **70**, 371 (1993).
- [57] J. Silk and M.S. Turner, *Phys. Rev. D* **35**, 419 (1986); L.A. Kofman, A.D. Linde, and J. Einsato, *Nature* **326**, 48 (1987).
- [58] D. La and P.J. Steinhardt, *Phys. Rev. Lett.* **62**, 376 (1991).
- [59] E.W. Kolb, *Physica Scripta* **T36**, 199 (1991).
- [60] M. Bucher A.S. Goldhaber, and N. Turok, hep-ph/9411206 (1994).
- [61] M.S. Turner and F. Wilczek, *Phys. Rev. Lett.* **65**, 3080 (1990); A. Kosowsky, M.S. Turner, and R. Watkins, *ibid* **69**, 2026 (1992).
- [62] M.S. Turner and L.M. Widrow, *Phys. Rev. D* **37**, 2743 (1988); B. Ratra, *Astrophys. J.* **391**, L1 (1992).

- [63] See e.g., A.D. Linde, *Phys. Lett. B* **158**, 375 (1985); D. Seckel and M.S. Turner, *Phys. Rev. D* **32**, 3178 (1985); M.S. Turner, A. Cohen, and D. Kaplan, *Phys. Lett. B* **216**, 20 (1989).
- [64] A. Albrecht et al, *Phys. Rev. Lett.* **48**, 1437 (1982); L. Abbott and M. Wise, *Phys. Lett. B* **117**, 29 (1992); A.D. Linde and A.D. Dolgov, *ibid* **116**, 329 (1992).
- [65] At first sight, first-order inflation might seem very different from slow-rollover inflation, as reheating occurs through the nucleation of percolation of true-vacuum bubbles. However, such models can be recast as slow-rollover inflation by means of a conformal transformation, and the analysis of metric perturbations proceeds as in slow rollover inflation. See e.g., E.W. Kolb, D. Salopek, and M.S. Turner, *Phys. Rev. D* **42**, 3925 (1990).
- [66] E.W. Kolb and M.S. Turner, *The Early Universe* (Addison-Wesley, Redwood City, CA, 1990), Ch. 8.
- [67] E.R. Harrison, *Phys. Rev. D* **1**, 2726 (1970); Ya.B. Zel'dovich, *Mon. Not. R. astr. Soc.* **160**, 1p (1972).
- [68] The material presented in this Section is a summary of M.S. Turner, *Phys. Rev. D* **48**, 3502 (1993); *ibid*, 5539 (1993).
- [69] J.M. Bardeen et al., *Astrophys. J.* **304**, 15 (1986).
- [70] D.H. Lyth and E.D. Stewart, *Phys. Lett. B* **274**, 168 (1992); E.D. Stewart and D.H. Lyth, *ibid*, **302**, 171 (1993).
- [71] L. Abbott and M. Wise, *Nucl. Phys. B* **244**, 541 (1984).
- [72] M. White, *Phys. Rev. D* **46**, 4198 (1992).
- [73] M.S. Turner, J.E. Lidsey and M. White, *Phys. Rev. D* **48**, 4613 (1993).
- [74] E.F. Bunn, D. Scott, and M. White, *Astrophys. J.* **441**, L9 (1995).
- [75] L. Abbott and M. Wise, *Nucl. Phys. B* **244**, 541 (1984); F. Lucchin and S. Mattarese, *Phys. Rev. D* **32**, 1316 (1985); R. Fabbri, F. Lucchin, and S. Mattarese, *Phys. Lett. B* **166**, 49 (1986).
- [76] D. La and P.J. Steinhardt, *Phys. Rev. Lett.* **62**, 376 (1989).
- [77] E.W. Kolb, D. Salopek, and M.S. Turner, *Phys. Rev. D* **42**, 3925 (1990).
- [78] E.J. Weinberg, *Phys. Rev. D* **40**, 3950 (1989); M.S. Turner, E.J. Weinberg, and L. Widrow, *ibid* **46**, 2384 (1992).

- [79] V. Belinsky, L. Grishchuk, I. Khalatanikov, and Ya.B. Zel'dovich, *Phys. Lett. B* **155**, 232 (1985); L. Jensen, unpublished (1985).
- [80] A.A. Starobinskii, *Sov. Astron.* **11**, 133 (1985).
- [81] A.D. Linde, *Phys. Lett. B* **108**, 389 (1982); A. Albrecht and P.J. Steinhardt, *Phys. Rev. Lett.* **48**, 1220 (1982).
- [82] For an overview of the cold dark matter scenario of structure formation see e.g., G. Blumenthal et al., *Nature* **311**, 517 (1984).
- [83] L. Knox and M.S. Turner, *Phys. Rev. Lett.* **73**, 3347 (1994).
- [84] M.S. Turner, J. Lidsey, and M. White, *Phys. Rev. D* **48**, 4613 (1993).
- [85] See e.g., C. Frenk, *Physica Scripta* **T36**, 70 (1991).
- [86] See e.g., J.P. Ostriker, *Ann. Rev. Astron. Astrophys.* **31**, 689 (1993); A. Liddle and D. Lyth, *Phys. Rep.* **231**, 1 (1993).
- [87] J. Bartlett et al., *Science* **267**, 980 (1995).
- [88] Q. Shafi and F. Stecker, *Phys. Rev. Lett.* **53**, 1292 (1984); S. Achilli, F. Occhionero, and R. Scaramella, *Astrophys. J.* **299**, 577 (1985); S. Ikeuchi, C. Norman, and Y. Zahn, *Astrophys. J.* **324**, 33 (1988); A. van Dalen and R.K. Schaefer, *Astrophys. J.* **398**, 33 (1992); M. Davis, F. Summers, and D. Schlegel, *Nature* **359**, 393 (1992); J. Primack et al., *Phys. Rev. Lett.* **74**, 2160 (1995); D. Pogosyan and A.A. Starobinskii, astro-ph/9502019.
- [89] M.S. Turner, G. Steigman, and L. Krauss, *Phys. Rev. Lett.* **52**, 2090 (1984); M.S. Turner, *Physica Scripta* **T36**, 167 (1991); P.J.E. Peebles, *Astrophys. J.* **284**, 439 (1984); G. Efstathiou et al., *Nature* **348**, 705 (1990); L. Kofman and A.A. Starobinskii, *Sov. Astron. Lett.* **11**, 271 (1985).
- [90] S. Dodelson, G. Gyuk, and M.S. Turner, *Phys. Rev. Lett* **72**, 3578 (1994); J.R. Bond and G. Efstathiou, *Phys. Lett. B* **265**, 245 (1991).
- [91] R. Cen, N. Gnedin, L. Kofman, and J.P. Ostriker, *ibid* **399**, L11 (1992); R. Davis et al., *Phys. Rev. Lett.* **69**, 1856 (1992); F. Lucchin, S. Mattarese, and S. Mollerach, *Astrophys. J.* **401**, L49 (1992); D. Salopek, *Phys. Rev. Lett.* **69**, 3602 (1992); A. Liddle and D. Lyth, *Phys. Lett. B* **291**, 391 (1992); J.E. Lidsey and P. Coles, *Mon. Not. R. astron. Soc.* **258**, 57p (1992); T. Souradeep and V. Sahni, *Mod. Phys. Lett. A* **7**, 3541 (1992).
- [92] See e.g., S. Parke, *Phys. Rev. Lett.* **74**, 839 (1995); C. Athanassopoulos et al, *ibid* **75**, 2650 (1995); J.E. Hill, *ibid*, 2654 (1995); K.S. Hirata et al, *Phys. Lett. B* **280**, 146 (1992); Y. Fukuda et al, *ibid* **335**, 237 (1994); R. Becker-Szendy et al, *Phys. Rev. D* **46**, 3720 (1992).

- [93] M. White, D. Scott, J. Silk, and M. Davis, astro-ph/9508009 (to appear in *Mon. Not. R. astron. Soc.*).
- [94] M.S. Turner, *Physica Scripta* **T36**, 167 (1991).
- [95] L. Krauss and M.S. Turner, astro-ph/9504003 [to appear in *Gen. Rel. Grav.* (1995)].
- [96] E.J. Copeland, E.W. Kolb, A.R. Liddle, and J.E. Lidsey, *Phys. Rev. Lett.* **71**, 219 (1993); *Phys. Rev. D* **48**, 2529 (1993); M.S. Turner, *ibid*, 3502 (1993); *ibid* **48**, 5539 (1993); A.R. Liddle and M.S. Turner, *Phys. Rev. D* **50**, 758 (1994).
- [97] A.R. Liddle, M.S. Turner, and M. White, to be submitted to *Phys. Rev. D* (1995).
- [98] L. Knox, *Phys. Rev. D* **52**, 4307 (1995).
- [99] M. Kamionkowski et al., *Astrophys. J.* **426**, L57 (1994); G. Jungman, M. Kamionkowski, A. Kosowsky, and D.N. Spergel, astro-ph/9507080 (1995).

This figure "fig1-1.png" is available in "png" format from:

<http://arXiv.org/ps/astro-ph/9703196v1>

This figure "fig1-2.png" is available in "png" format from:

<http://arXiv.org/ps/astro-ph/9703196v1>

This figure "fig1-3.png" is available in "png" format from:

<http://arXiv.org/ps/astro-ph/9703196v1>

This figure "fig1-4.png" is available in "png" format from:

<http://arXiv.org/ps/astro-ph/9703196v1>

This figure "fig1-5.png" is available in "png" format from:

<http://arXiv.org/ps/astro-ph/9703196v1>

This figure "fig1-6.png" is available in "png" format from:

<http://arXiv.org/ps/astro-ph/9703196v1>

This figure "fig1-7.png" is available in "png" format from:

<http://arXiv.org/ps/astro-ph/9703196v1>

This figure "fig1-8.png" is available in "png" format from:

<http://arXiv.org/ps/astro-ph/9703196v1>